**ADDIS ABABA UNIVERSITY**

**ADDIS ABABA INSTITUTE OF TECHNOLOGY**

**SCHOOL OF CIVIL AND ENVIRONMENTAL ENGINEERING**




# ASSESSMENT OF DEGRADATION ON THE INTERFACE OF CONCRETES CAST AT DIFFERENT TIMES SUBJECTED TO CYCLIC SHEAR LOADING IN DRY AND MOIST CONDITION

---

**A Thesis in Structural Engineering**

**By Yonas Solomon**

**March 19, 2018**

**Addis Ababa**

**A Thesis**

**Submitted in Partial Fulfilment of the Requirements for the Degree of Master of Science**

The undersigned have examined the thesis entitled **'Assessment of Degradation on The Interface of Concretes Cast at Different Times Subjected to Cyclic Shear Loading in Dry and Moist Condition'** presented by **Yonas Solomon**, a candidate for the degree of **Master of Science** and hereby certify that it is worthy of acceptance.

| | | |
|---|---|---|
| Dr. Esayas Gebreyouhannes | | |
| Advisor | Signature | Date |
| Dr.-Ing. Girma Zerayohannes | | |
| Internal Examiner | Signature | Date |
| Dr.-Ing. Adil Zekaria | | |
| External Examiner | Signature | Date |
| Dr. Agizew Nigussie | | |
| School Dean | Signature | Date |

# ACKNOWLEDGMENT

I would like to express my deepest gratitude and respect to my advisor and mentor Dr. Esayas G/youhannes, for his incredible support and advice. It was an honor working with someone so brilliant and humble. Not only did he guide me on the work with uttermost rational thinking, but he also triggered a whole new attitude on me towards research. I would also like to thank him for providing me with valuable instruments for the laboratory work.

I would like to give an immense credit to my friend and colleague Ato Mohammed Sirage. This work would not have been possible without his imperative help. His contribution of bringing novel ideas to the table cannot go unmentioned. He has also been there in every step of the laboratory and editorial work as well.

I would like to acknowledge Ato Firesenay Zerabruk who paved the way for works with the push-off specimens at the laboratory. Formworks used for the samples were prepared by him during his work.

I would like to thank Dr. Abreham Gebre, Dr.-Ing. Adil Zekaria and Dr.-Ing. Girma Z/youhannes for their continuous supervision and concern.

I would also like to acknowledge the people who made the physical laboratory work simpler with their valuable assistance: Abel, Binyam, Demis, Fikru, Masresha and Wibet.

My heartfelt gratitude goes to Ato Leamlak and Ato Balem for providing me with reinforcement bars for free and giving me a well-needed encouragement.

I would also like to express my appreciation for my friend Mariamawit weldegabrial for taking her time to edit the paper. I am also grateful to my colleagues at AAiT especially my office mates and my friends for their constant encouragement and moral support.

Lastly, I would like to thank all my family members for their prayer and unconditional support which is my driving force in life.

# TABLE OF CONTENT

**ACKNOWLEDGMENT** ..... **I**

**TABLE OF CONTENT** ..... **II**

**LIST OF TABLES** ..... **IV**

**LIST OF FIGURES** ..... **V**

**ABSTRACT** ..... **VIII**

**1 INTRODUCTION** ..... **1**

1.1 General Background of the Study ..... 1

1.2 Statement of the Problem ..... 2

1.3 Objective of the Study ..... 2

1.4 Scope of the Study ..... 3

1.5 Methodology ..... 3

1.6 Organization of the Thesis ..... 3

**2 LITERATURE REVIEW** ..... **4**

2.1 Shear Transfer Mechanism ..... 4

2.1.1 Adhesive Bond ..... 4

2.1.2 Friction ..... 5

2.1.3 Dowel Action: ..... 6

2.2 Interaction of Shear Transfer Mechanisms ..... 6

2.3 Factors Affecting Shear Transfer Capacity ..... 7

2.4 Shear Transfer under Cyclic Loading ..... 12

2.5 Outstanding Issues and Research Needs ..... 13

**3 EXPERIMENTAL PROGRAM** ..... **15**

3.1 Choice of a Test Specimen ..... 15

3.2 Scope of the Experimental Program ..... 18

3.3 Material ..... 20

3.3.1 Concrete: ..... 20

3.3.2 Cement ..... 20

3.3.3 Coarse Aggregate: ..... 20

3.3.4 Fine Aggregate: ..... 20

3.3.5 Reinforcement ..... 21

3.4 Specimen Preparation ..... 22

3.5 Test Setup and Instrumentation ..... 27

**4 EXPERIMENTAL RESULTS AND DISCUSSION** ..... **38**

4.1 Results of Monolithically Cast Specimens....38
4.2 Results of Specimens with the Interface in Dry Condition....40
4.2.1 Specimen DM....40
4.2.2 Specimen DC-75....44
4.2.3 Specimen DC-70....47
4.2.4 Comparison amongst the Dry Specimen....49
4.3 Results of Specimens with the Interface in a Moist Condition....50
4.3.1 Specimen MM....50
4.3.2 Specimen MC-82....52
4.3.3 Specimen MC-60....54
4.3.4 Comparison amongst the Moist Specimens....56
4.4 Comparison between the Monolithically Cast Specimens and Specimens with an Interface....57
4.5 Comparison between Moist and Dry Specimens....58
4.6 Summary of the Experimental Result....61
**5 FINITE ELEMENT MODELING....62**
5.1 About the Software....62
5.2 Specimens Modeled....62
5.3 Modeling the Specimens....62
5.3.1 Concrete:....62
5.3.2 Reinforcement:....63
5.3.3 Bond Element....63
5.3.4 Support Condition....64
5.4 Results of the Monotonically Loaded Specimen....65
5.5 Results of the Specimen with an Interface....65
**6 CONCLUSION AND RECOMMENDATION....67**
6.1 Conclusions....67
6.2 Recommendation....68
**REFERENCE....69**

# LIST OF TABLES

Table 3-1: Properties of coarse aggregate used ..... 20
Table 3-2: Properties of fine aggregate used ..... 21
Table 3-3: Specimen designation and compressive strength ..... 25
Table 4-1: Results of monolithically cast specimens ..... 61
Table 4-2: Results of specimens with an interface ..... 61
Table 5-1: Properties of concrete used in the model ..... 62
Table 5-2: Reinforcement property used in the model ..... 63
Table 5-3: Bond element parameters ..... 64

# LIST OF FIGURES

Figure 2-1: Load versus displacement curve for an interface with concrete cast at different times (E.N.B.S. Julio et al., 2010) ..... 4
Figure 2-2: Frictionless saw tooth ramp model of friction mechanism (Birkeland, H. W.; Birkeland, P. W.,1966) ..... 5
Figure 2-3: Dowel action mechanism (Walraven, 1980) ..... 6
Figure 2-4: Different forms of bar bending (Walraven, 1980) ..... 6
Figure 2-5: Bond strength variation with different types of surface roughening techniques (E.N.B.S. Julio et al., 2004) ..... 8
Figure 2-6: Evolution of concrete shrinkage strain (E.N.B.S. Julio and Pedro M D Santos, 2011). ..... 9
Figure 2-7: Bond strength for varying curing condition of interface (E.N.B.S. Julio and Pedro M D Santos, 2011). ..... 10
Figure 2-8: Arrangement of restraint plates and bars on the specimens (Walraven, 1997) ..... 11
Figure 3-1: Samples used to investigate interface shear transfer ..... 15
Figure 3-2: Modifications to the push-off sample ..... 16
Figure 3-3: Preliminary model of the Push-off specimen using VecTor3 ..... 17
Figure 3-4: Selected push-off specimen configuration ..... 17
Figure 3-5: Reinforcement layout of the selected push-off specimen ..... 18
Figure 3-6: Fine and coarse aggregates packed in a plastic bag ..... 21
Figure 3-7: Stress-strain diagram of reinforcement crossing the interface (Zerabruk, 2015) ..... 22
Figure 3-8: Metal Formwork ..... 23
Figure 3-9: Mixer machine ..... 23
Figure 3-10: Surface finish of the interface ..... 24
Figure 3-11: Plating of the push-off specimen ..... 25
Figure 3-12: Trial test set up and instrumentation ..... 28
Figure 3-13: Load rate applied using an automatic compression machine ..... 29
Figure 3-14: Second trial test set up and instrumentation ..... 30
Figure 3-15: Load rate achieved using a manually operated hydraulic jack ..... 30
Figure 3-16: Displacement versus load with a displacement measured by transducers ..... 31
Figure 3-17: Rosette strain gauge ..... 32
Figure 3-18: Application of strain gauges on a grooved cube sample ..... 32
Figure 3-19: Load by a compression machine ..... 33
Figure 3-20: Load by a jack ..... 33

Figure 3-21: Strain versus load diagram of a cube specimen for the load applied using jack.33
Figure 3-24: Poisson's ratio .....34
Figure 3-22: Strain versus load graph for a cube specimen using a compression machine ....34
Figure 3-23: Mohr's circle for selected points.....35
Figure 3-25: Final test set up and instrumentation for specimens loaded in dry condition.....36
Figure 3-26: Test set up for specimens tested in moist condition.....37
Figure 4-1: Cracked surface of monolithically cast specimens (a) monotonically loaded specimen; (b) cyclically loaded specimen .....39
Figure 4-2 Average confining stress to load applied of monolithically cast specimens at failure cycle.....40
Figure 4-3: Orientations and symbols used in the charts.....41
Figure 4-4: Average shear stress to strain curve of specimen DM (a) all average strain of the interface; (b) horizontal strain at the front and back side; (c) Vertical strain at the front and back side; (d) strain at an angle of $45^o$ at the front and back side; (e) shear strain at the front and back side up to peak stress .....42
Figure 4-5: Orientation of shear deformation .....43
Figure 4-6: Possible eccentric loading.....43
Figure 4-7: Result of specimen DC-75 (a) Average strain of the interface to average shear stress; (b) Evolution of horizontal strain at the front and back side with number of cycle; (c) Evolution of Vertical strain at the front and back side with number of cycle; (d) Evolution of strain at $45^o$ at the front and back side with number of cycle; (e) Evolution of shear strain at the front and back side with number of cycle .....46
Figure 4-8: Shear stress – strain curve of specimen DC-75.....46
Figure 4-9: Result of specimen DC-70 (a) Average strain of the interface to average shear stress; (b) Evolution of horizontal strain at the front and back side with number of cycle; (c) Evolution of Vertical strain at the front and back side with number of cycle; (d) Evolution of strain at $45^o$ at the front and back side with number of cycle; (e) Evolution of shear strain at the front and back side with number of cycle .....48
Figure 4-10: Shear stress – strain curve of specimen DC-70.....48
Figure 4-11: Average shear stress to strain curve of all specimens tested in dry condition. (a) Horizontal and vertical strain; (b) Strain at $45^o$; (c) Shear strain.....49
Figure 4-12: (a) Shear stress – strain curve of all specimens tested in dry condition; (b) Evolution of shear strain with number of cycles of all specimens in dry condition. .....50

Figure 4-13: Average shear stress to strain curve of specimen MM (a) all average strain of the interface; (b) horizontal strain at the front and back side; (c) Vertical strain at the front and back side; (d) strain at an angle of $45^o$ at the front and back side; (e) shear strain at the front and back side ..... 52
Figure 4-14: Result of specimen MC-82 (a) Evolution of horizontal strain at the front and back side with number of cycle; (b) Evolution of Vertical strain at the front and back side with number of cycle; (c) Evolution of strain at $45^o$ at the front and back side with number of cycle; (d) Evolution of shear strain at the front and back side with number of cycle ..... 53
Figure 4-15: Shear stress – strain curve of specimen MC-82 ..... 54
Figure 4-16: Result of specimen MC-60 (a) Evolution of horizontal strain at the front and back side with number of cycle; (b) Evolution of Vertical strain at the front and back side with number of cycle; (c) Evolution of strain at $45^o$ at the front and back side with number of cycles; (d) Evolution of shear strain at the front and back side with number of cycles ..... 55
Figure 4-17: Shear stress – strain curve of specimen MC-60 ..... 55
Figure 4-18: Average shear stress to strain curve of all specimens tested in a moist condition. (a) Horizontal and vertical strain; (b) Strain at $45^o$; (c) Shear strain ..... 56
Figure 4-19: (a) Shear stress – strain curve of all specimens tested in moist condition; (b) Evolution of shear strain with a number of cycles of all specimens in a moist condition. ..... 57
Figure 4-20: (a) Cracked surface of monolithically cast specimens (a) Cracked surface of the specimen with an interface tested in dry condition; (b) Cracked surface of the specimen with an interface tested in moist condition ..... 58
Figure 4-21: Average shear stress to strain curve of all specimens (a) Horizontal and vertical strain; (b) Strain at $45^o$; (c) Shear strain ..... 59
Figure 4-22: (a) Shear stress – strain curve of all specimens; (b) Evolution of shear strain with number of cycles of all specimens. ..... 60
Figure 5-1: (a) Model of the entire specimen; (b) Internal reinforcement layout; (c) Bond element for specimens with an interface. ..... 63
Figure 5-2: Average tensile strain of confining bars (experimental Vs DuCOM-COM3) ..... 65
Figure 5-3: Failure envelope ..... 66
Figure 5-4: Comparison of experimental and model results of the monotonically loaded specimen ..... 66

# ABSTRACT

Understanding the nature of shear transfer across an interface between old and new concrete is essential since the formation of this joint compromises the shear resistance capacity of a member as compared to a monolithically cast concrete. This kind of interfaces can be encountered in different areas of engineering. For instance, in various strengthening and repair works, when structural members cannot be cast at once due to work interruptions, when the construction method is a mixture of pre-casting and casting in place, rigid pavement construction and so on. In this paper, the degradation nature of the type of interface mentioned above is studied for cyclic shear loading in a dry and moist condition.

Nine push-off specimens were cast on the experimental program. Three specimens were cast monolithically and tested in a dry condition while the others were made to have an interface. The surface of the substrate concrete was left as cast without any roughening. Three specimens were tested in a dry condition while the other three were tested in a moist condition. The specimens were tested while submerged in water in a tanker specially made for the test. Monotonic and one directional cyclic load at varying amplitude was considered for each set of specimens.

A novel instrumentation scheme to measure the deformation at the interface was used. Three strain gauges were placed on each side of the interface in three different directions from which shear strain was calculated. This setup was used due to the rigid behavior of the interface before de-bonding occurs.

The experimental program indicated that the presence of water pronouncedly accelerated the degradation of the interface for cyclic loading. A solid conclusion could not be made on the difference of degradation nature of concrete with and without an interface introduced with the limited number of specimens tested. The existence of a joint at the interface seemed to drastically reduce the shear transfer capacity for monotonic loading condition. A reduction of capacity up to 36.6% was observed.

A model of the specimen with and without an interface was simulated on a nonlinear finite element analysis program DuCOM-COM3 for monotonic loading. The ultimate load was captured in a fair proximity with the available interface model.

# 1 INTRODUCTION

## 1.1 General Background of the Study

Reinforced concrete structures are designed to withstand stresses resulting from compression, tension, and shear. When designing structures, it is a good practice to avoid forming members that are critical to fail in shear. This is because shear failure by its nature is brittle and does not give any warning before failure. In designing structures to dissipate energy during vibration by forming plastic hinges, as done in capacity design method, sections are over strengthened for shear capacity in order to avoid brittle failure before the formation of hinges.

However, there are situations during construction that could compromise the shear-resisting capacity of members. One of these situations is the formation of construction joints. These joints are formed when a fresh concrete is cast over a concrete that has already set. Adhesive bond of concrete at the interface drops as compared to a monolithic concrete. The interface between the concretes of different ages could be a weak zone for shear resistance.

Formation of construction joints is not uncommon. There are several reasons for the formation of construction joints. To mention a few:

- Various strengthening and repair works involve casting a fresh concrete overlay on an old concrete substrate that has already set. For example columns, bridge decks and beams could be strengthened with an additional concrete overlay forming a construction joint at the interface.
- While casting beams or slabs, the work might get interrupted due to the failure of machines, power outage, not having the capacity to cast all area in one day and so on. If the concrete is left alone for beyond its setting time when the casting process is commenced, the formation of construction joint is inevitable.
- When the construction method is a mixture of pre-casting and casting in place. For instance, using pre-cast beams and cast in place slabs as may be done during construction of bridges, these joints could be formed.
- During construction of rigid pavements, concrete is not cast monolithically along the entire length of the road, rather construction joints are formed at a certain interval.
- Construction joints can also be formed to correct construction errors. Some practical cases are a deflection of slabs due to the settlement of scaffoldings, forgetting to place

ducts before casting and so on. If some part of the structure is demolished and reconstructed, then construction joints would be formed at those locations.

Furthermore, application of cyclic type of load degrades the shear carrying capacity of concrete member elements. Situations like vehicle crossing a bridge and earthquake can induce such type of loading on structures. The combination of these two scenarios – formation of construction joints and imposition of cyclic loads can significantly undermine the capacity of structural members.

Construction joints serve as a conduit in the presence of water. This could significantly reduce the shear transfer capacity of an interface especially after cracking of the concrete has begun. The water washes out fine particles at the interface which are involved in the shear transfer mechanism resulting in a reduced shear capacity of the interface.

In this study, the degradation behavior of the interface between old and new concrete was investigated under different amplitudes of cyclic shear loading before total de-bonding of the interface occurred. The effect of water was also a subject of investigation in the degradation nature of the interface.

## 1.2 Statement of the Problem

It is clear that the formation of construction joints is unavoidable and conditions creating cyclic loads are present, so it is important to understand the degrading behavior of the interface in order to properly design them to withstand expected loads. Incorporation of the effect of environmental factors like water on the interface will broaden the present understanding of shear transfer mechanism at the interface.

## 1.3 Objective of the Study

The objective of the study is to investigate the degradation behavior of interface shear transfer between concretes cast at different times before complete de-bonding of the interface occurs while incorporating the effect of the presence of water.

## 1.4 Scope of the Study

Shear is transferred across an interface by three major mechanisms that are mobilized at different load stages. These are adhesive bonding, friction and dowel action. Adhesive bonding is the first mechanism to be dominant. In this stage of shear transfer, the interface is stiff and can carry stress at low strain amounts. After the interface de-bonds, i.e. the interface fully cracks, the latter two mechanisms come into play. This point of de-bonding is usually the ultimate shear stress that can be carried by the interface. This study focuses on the stage of load transfer before complete de-bonding of the interface occurs.

At the stage of load transfer mechanism, different conditions affect the behavior of the interface. The roughness of the interface, concrete strength, curing condition (environmental condition), a difference of age between the overlay concrete and substrate concrete, confining stress perpendicular to the shear plane, reinforcement parallel and perpendicular the interface and type of loading are the major factors that affect the shear transfer capacity. This study tries to address the effect of loading and environmental condition i.e. presence of water at the interface while keeping the other factors constant.

## 1.5 Methodology

In order to meet the objective of the research three major steps were taken. First literature related to the topic was thoroughly reviewed. Using the existing literature as an input, an experimental program was set up to best study the topic at hand. A push off sample was used to create a shear critical interface. Finally, analytical simulation using non-linear finite software element incorporating outputs of the experimental program was done.

## 1.6 Organization of the Thesis

The paper consists of a total of six chapters. Chapter two of the paper highlights previous works on shear transfer mechanism of constriction joints. In chapter three the detail of the experimental program is discussed. The process of refining the test set up and instrumentation is shown in this chapter. Chapter four shows the results from the experimental program accompanied with analysis and discussion. In chapter five results from the experiment are used in the nonlinear analysis software DuCOM-COM3. Finally, chapter six gives the conclusion and recommendation

# 2 LITERATURE REVIEW

## 2.1 Shear Transfer Mechanism

There are different mechanisms involved in the shear transfer process at the interface between concrete cast at different times. Different studies show that these mechanisms act simultaneously with varying contribution at different loading stages of the interface. The shear transfer mechanisms include Adhesive bond, friction, and dowel action.

### 2.1.1 Adhesive Bond

Adhesive bond is induced due to the chemical bond between the newly casted concrete and the concrete that has already set. This chemical bonding is also known as Van der Waals force.

In the study conducted at the University of Porto to investigate the cyclic behavior of cracked interface with concrete cast at different times (Figueira et al., 2015), specimens with a pre-crack induced at their interface exhibited a reduced shear capacity than specimens without an existing crack. This reduction is attributed to the loss of adhesion due to the cracked interface.

Adhesion is the first mechanism to be developed in the shear transfer process. It also has a rigid behavior. At low values of slip, a large amount of stress is achieved due to this mechanism. After de-bonding, a considerable reduction in strength is observed as shown in Figure 2-1. (Júlio, E. N. B. S et al., 2010).

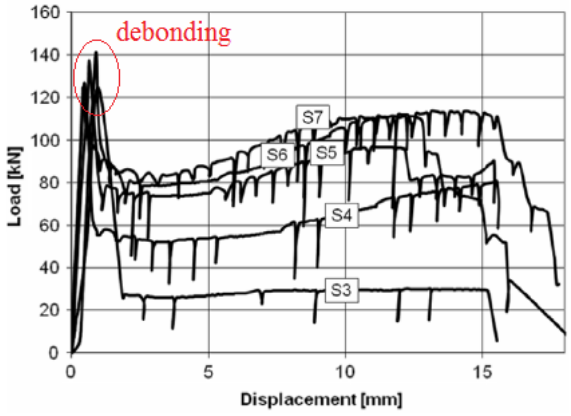



**Figure 2-1: Load versus displacement curve for an interface with concrete cast at different times (E.N.B.S. Julio et al., 2010)**

### 2.1.2 Friction

This mechanism occurs when the shear plane is rough and there exists a normal or clamping force perpendicular to the plane. The clamping force might result due to an embedded rebar crossing the interface or due to an external force applied.

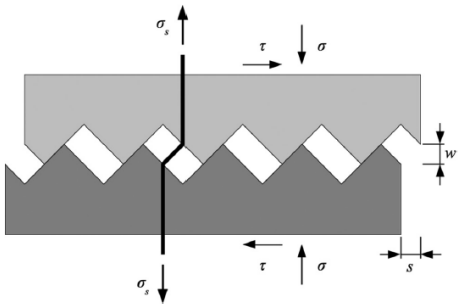



**Figure 2-2: Frictionless saw tooth ramp model of friction mechanism (Birkeland, H. W.; Birkeland, P. W.,1966)**

When two surfaces with a rough plane slide against one another, there will be a lateral opening w, in addition to the slip movement. If reinforcement exists perpendicular to the interface, a tensile stress will be induced in the rebar which in turn induces a clamping stress on the interface. This phenomenon mobilizes friction resistance. This concept was first utilized by Birkeland H.W and Birkeland P.W in 1966 and they came up with the shear friction theory to predict the ultimate stress for a cracked interface. Equations to predict the ultimate shear capacity of interfaces is given on design codes mainly based on this theory.

**Equation 2-1: shear friction equation**

$$v_u = \rho . f_{syd} . \tan\phi$$

### 2.1.3 Dowel Action:

Dowel action is defined as the capacity of reinforcement to transfer forces perpendicular to their axis. The resistance is developed by the bending of the reinforcement.

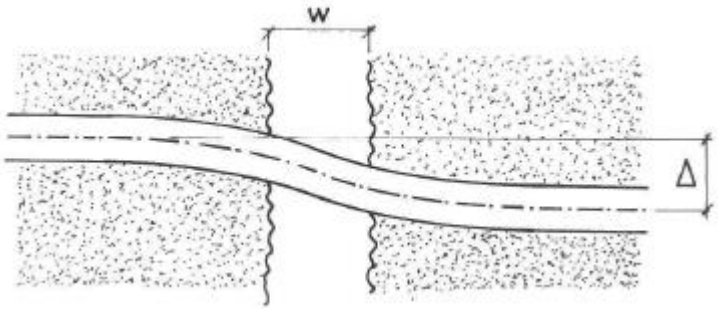



**Figure 2-3: Dowel action mechanism (Walraven, 1980)**

The total deflection of the bar is the sum of the deflection of the free bar and the bar embedded in the concrete. The deformation of the bar could take the forms shown in Figure 2-4.i.e. load transfer by bending, load transfer by pure shear and load transfer by kinking.

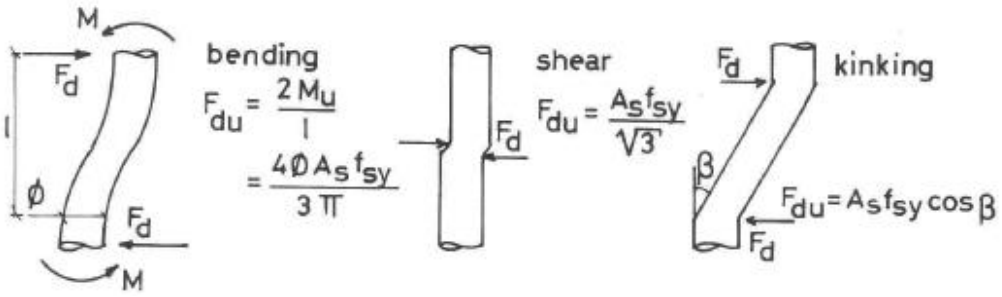



**Figure 2-4: Different forms of bar bending (Walraven, 1980)**

## 2.2 Interaction of Shear Transfer Mechanisms

The three mechanisms involved in the shear transfer process are not mobilized with the same magnitude throughout the loading stage. Adhesion is the first mechanism to be developed. The deformation at the interface at this stage is small and elastic behavior is dominant.

With an increased slip and on set of crack at the interface, Adhesion bonding disappears and friction and dowel action become dominant in the load transfer mechanism. The contribution of the two mechanisms is dependent on the roughness of the interface, stress normal to the

interface and anchorage of the reinforcement bar crossing the interface. On a study conducted by mattock (1969), he showed that dowel action has a small contribution on un-cracked concrete. He prepared monolithically casted samples in which the rebar on some of the specimen were put in rubber sleeves to diminish dowel action. The two sets of specimens showed similar strength despite the loss of dowel action. He prepared similar samples for cracked specimens as well and the results showed up to 34% reduction in strength when dowel action was eliminated. From this, it is possible to conclude that dowel action becomes significant after a crack has formed on the interface.

It is also possible to see the mechanism in Figure 2-1. At the point of de-bonding, there is a sudden drop in stiffness and as the load is increased, the graph starts to go up because of the mobilization of friction and dowel action. Similar behavior is reported in other studies as well (Figueira et al., 2015).

## 2.3 Factors Affecting Shear Transfer Capacity

The mechanisms mentioned in the previous section are influenced by different factors. It is important to study these factors in order to control the experimental program in the paper. Factors studied by different researchers are:

A. Characteristic of roughness
B. Characteristic of concrete
C. Curing condition
D. Difference of age
E. Characteristic of reinforcement
F. Stress perpendicular to the shear plane
G. Type of loading

### A. Characteristic of Roughness

The roughness of the interface is an important parameter in the shear transfer mechanism. It affects adhesion bonding, friction and dowel action.

As the roughness of the interface increases, the adhesive bonding also increases (Júlio, E. N. B. S et al., 2004). Different types of surface treatments were applied to an interface. The roughening techniques studied were sand-blasting, chipping and steel brushing. Slant shear

test was conducted to evaluate the bond strength. The surface that was sand-blasted showed the maximum bond strength as shown in Figure 2-5.

Slant shear test results

| Situations considered | Substrate surface treatment | Bond strength in shear (MPa) | Variation co-efficient (%) |
|---|---|---|---|
| 1 | As-cast against steel formwork | 1.30 | 33.85 |
| 2 | Wire-brushing | 10.67 | 8.90 |
| 3 | Partially chipped | 6.24 | 20.67 |
| 4 | Partially chipped and pre-wetted | 6.64 | 13.10 |
| 5 | Sand-blasting | 14.13 | 8.56 |

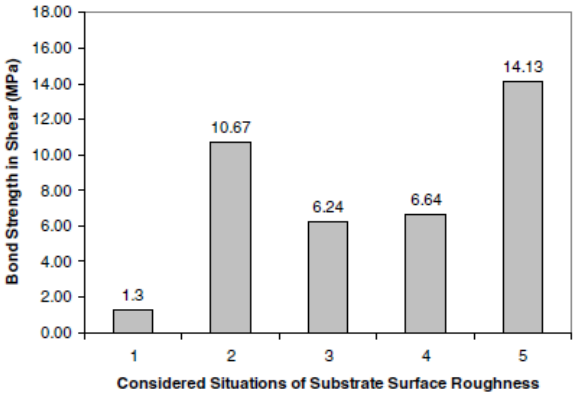



**Figure 2-5: Bond strength variation with different types of surface roughening techniques (E.N.B.S. Julio et al., 2004)**

On another paper, the authors used digital image processing to quantify the roughness that is created by sand-blasting, wire brushing and as-cast surface (Júlio, E. N. B. S et al., 2007). After capturing the surface profile, the authors used different criteria to quantify the roughness. It was shown that the bond strength was directly proportional to the amount of roughness parameter assigned.

Roughness also affects the amount of friction resistance developed between the surfaces. The roughness and a normal force perpendicular to the interface are the parameters that influence friction as can be seen in the shear friction formula.

The effect of roughness on dowel action was discussed by (Figueira et al., 2015). When the roughness of the interface increases, the specimen tends to split more than it slips. This transverse opening of the interface tends to put the reinforcement in tension rather than bending it. So for a rough interface, dowel action may not be mobilized significantly before failure of the interface. On the other hand, for a very smooth interface, slipping movement is dominant than splitting so the contribution of dowel action becomes significant.

### B. Characteristic of Concrete

For cracked concrete, it has been shown that as the compressive strength of concrete increases the shear capacity of the interface also increases (Walraven, 1997; mattock, 1969). However on a study conducted by mattock (1969), he found that for a fixed amount of $\rho f_y$ (product of reinforcement ratio and yield strength of reinforcement crossing the interface)

present across the interface, there is an upper value of concrete compressive strength in which concrete strength above that point would not enhance the shear capacity, But for compressive strength below this point, the shear capacity reduces.

### C. Curing Condition:

For an interface with concretes cast at different times, curing condition is a major factor that influences bond strength. This is due to differential shrinkage of the two surfaces (E.N.B.S. Julio and Pedro M D Santos, 2011). On the Study, one set of samples were cured in the laboratory and another set of samples were cured outside with varying solar radiation, rain and wind. The variation of environmental condition was more severe on the outside. The curing condition was maintained throughout the life of the specimens. Shrinkage strain was monitored for the two curing conditions as well.

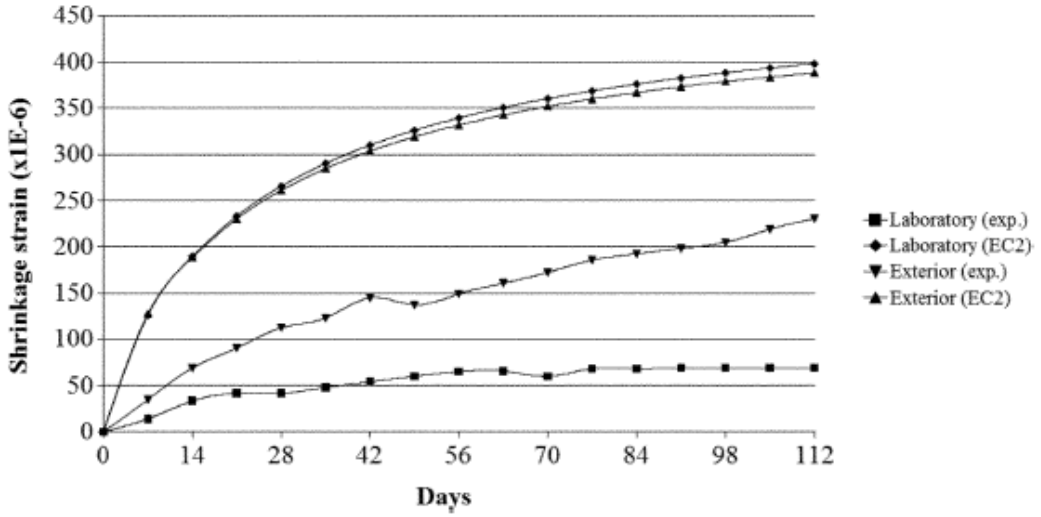



**Figure 2-6: Evolution of concrete shrinkage strain (E.N.B.S. Julio and Pedro M D Santos, 2011).**

The shrinkage stress was higher for the specimens stored on the outside hence during testing these samples showed lesser shear capacity (Figure 2-6). The samples labeled “L” were stored in the laboratory and samples labeled “E” were stored outside on Figure 2-7.

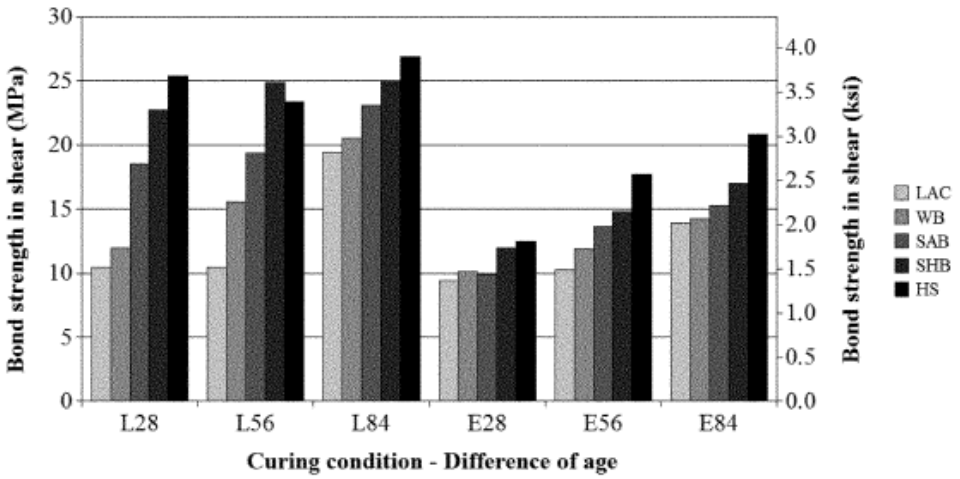



**Figure 2-7: Bond strength for varying curing condition of interface (E.N.B.S. Julio and Pedro M D Santos, 2011).**

**D. Difference of Age:**

The time gap between casting the two parts of the specimen also has an effect on the bond strength. On the same study conducted by Julio (2011), time gapes of 28, 56 and 84 days were studied. As the time difference increased the bond strength seemed to increase.

**E. Characteristic of Reinforcement:**

1. Reinforcement Perpendicular to the Shear Plane:

The reinforcement crossing the shear plane plays a major role in the shear transfer process. Amount of reinforcement, orientation of reinforcement, anchorage and whether the reinforcement is embedded in the concrete or tied externally are the factors that should be considered.

2. Amount of Reinforcement:

The effect of the amount of reinforcement crossing shear plane was studied by mattock (1969) for a monolithically casted concrete and for cracked concrete. Mattock found that when the amount of reinforcement is significantly high, cracked concrete shows similar behavior as the monolithically casted concrete

So in order to compare the effect of construction joints with monolithically casted concrete, the amount of reinforcement should not be high so as to not mask the effect of the construction joint.

3. Orientation of Reinforcement:

The effect of bar inclination was studied by Walraven (1997). He studied it for reinforcement embedded in concrete for pre-cracked shear plane. He found that as the inclination increases, the shear strength of the interface decreases.

4. Way of Placement of Reinforcement:

In practical situations, reinforcement is placed inside concrete on shear planes. For research purpose, it is sometimes desirable to place the bars externally. This is because when the reinforcement is embedded, accurately measuring the strain of the reinforcement becomes a challenge. In addition, the bond property between concrete and reinforcement might vary for the different samples. Placing the bar externally helps to avoid this constraints.

Bars are also placed externally in order to eliminate the effect of dowel action to study the shear transfer mechanism of concrete. Walraven (1997) applied this method of specimen preparation and confirmed it reduces the dowel effect to a negligible value (Figure 2-8). Mattock (1969) also tried to eliminate the effect of dowel action by placing a rubber sleeve around the reinforcement inside the concrete.

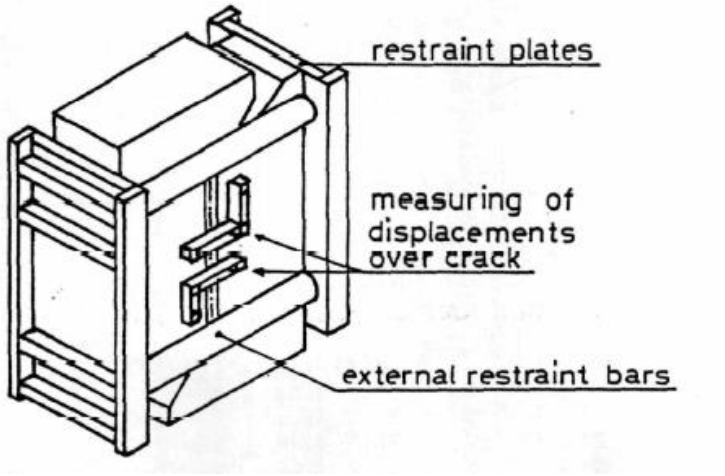



**Figure 2-8: Arrangement of restraint plates and bars on the specimens (Walraven, 1997)**

5. Reinforcement Parallel to the Shear Plane:

Reinforcement parallel to and found in the vicinity of the shear plane contributes to the shear transfer strength (Thomas T.C Hsu, S. T Mau, and Bin Chen, 1987). An analysis based on truss model with softened compression stress-strain relation for concrete was used to analyze

shear transfer strength in initially un-cracked concrete. A critical zone was identified and analyzed. With this, the contribution of reinforcement parallel to the shear plane was shown.

**F. Stress Perpendicular to the Shear Plane:**

It can be easily understood from friction theory that if the normal stress perpendicular to the interface increases, shear resistance also increases.

**G. Type of Loading:**

Whether the load is static, cyclic or sustained has an effect on the behavior of structures. This holds true for shear planes as well. Effect of cyclic loading on shear transfer mechanism off interfaces is discussed in the next section.

## 2.4 Shear Transfer under Cyclic Loading

Studies on the cyclic shear response of interfaces started emerging in the 80's (Vintzileou and Tassios, 1987). Reports have also been made on the topic in recent times as well (Figuerie, 2015). Studies have been conducted on both cracked interface and interface that has no pre-crack but constructed by casting fresh concrete on an old one. Studies have focused on the response of the two shear transfer mechanisms that is friction and dowel action. Not a lot of focus is given to Adhesive bonding.

Vintzileou and Tassios (1987) studied dowel action behavior under cyclic shear loading. The specimen used in the experiment was modified to allow shear transfer through dowel action only. Significant degradation was observed during the experiment. The amplitude of cyclic loading was not investigated in depth.

Surface preparation, amount and depth of embedment, reinforcement detailing and compressive strength of concrete were investigated under cyclic shear loading for an interface with concrete cast at different times (Bass et al, 1989). It was observed that deeper embedment and increased number of bars crossing the interface increased the shear transfer capacity of the interface. Here again, the effect of the amplitude of cyclic loading was not deeply investigated. Similar detail study on a different specimen was also conducted in recent time (palierani et al, 2012).

A study on cracked interface shear transfer was done entailing friction under cyclic shear loading (Gebreyouhannes et al, 2008). Load amplitude and load pattern were shown to have an effect on the shear transfer process. In addition, the downward flow of water on the

interface was investigated under cyclic loading. It was found that water exposure speeds up shear degradation.

Dowel action and friction mechanism were studied under cyclic shear loading on a cracked interface in which the concretes were cast at different times. The effect of load amplitude on the behavior of the two mechanisms was discussed. For low amplitude cyclic shear loading, the steel failed due to fatigue and dowel action was not mobilized significantly. The steel bars ruptured during failure. For high amplitude cyclic loading, dowel action is well mobilized. The concrete cover was damaged at the time of failure and the steel bars did not rupture.

## 2.5 Outstanding Issues and Research Needs

It is justifiable to address the shear transfer mechanism of a cracked interface in depth since concrete could crack under environmentally induced loads over time; however, the behavior before crack formation is also fundamental. The adhesive strength of concrete becomes critical for concrete structures where serviceability cannot be compromised. Considering nuclear power plant concrete structures and water retaining structures, crack formation can have a serious consequence. If construction joint exists in such kind of structures, the adhesive bond strength will be reduced. Adhesive bond is also critical for concrete structures exposed to an aggressive environmental condition like water and chlorine ion. Formation of crack could allow migration of these materials to the reinforcement and ultimately cause the structure to be vulnerable.

Another important parameter is the presence of water. The compressive and tensile strengthening effect of water in pores of concrete for high load rate has been reported in literature (Kaji, T., & Fujiyama, C., 2014; Ross, C. A. et al., 1996). For static loading condition, water seems to enhance the stiffness of concrete at lower load levels due to the development of pore water pressure. But ultimately the water enhances micro-crack propagation and result in a reduced ultimate strength (Zheng, D., & Li, X. X., 2011). Few papers have tried to address the adverse effect of water under fatigue compression loading (Karanfilov, T. S., 1967; Matsushita, H., & Onoue, K., 2006). However, the interaction between water and construction joints on shear capacity of concrete is not discussed in literature.

This paper will investigate the cyclic shear degradation of adhesive bonding between concretes cast at different time before de-bonding of the interface. Even though this

mechanism has a rigid nature, its degradation nature should be scrutinized on this weak construction joints. Furthermore, the degradation nature of the interface is evaluated with the presence of water.

# 3 EXPERIMENTAL PROGRAM

In this chapter, the details of the experimental program undertaken to investigate adhesive bond degradation between concrete cast at different times at the Construction Material laboratory of Addis Ababa Institute of technology is presented. A specimen suitable to investigate interfaces between concrete cast at different times for a condition critical to shear was selected. The parameters under investigation along with the set of specimens prepared are discussed. The process of specimen preparation is also briefly presented. The different step taken to reach the final test set up and instrumentation is discussed.

## 3.1 Choice of a Test Specimen

The experimental program aims to investigate the adhesive bond degradation between concrete interfaces cast at different times as a result of cyclic shear loading in dry and moist condition. The specimen should allow the application of shear stress on the interface possibly excluding the other shear transfer mechanisms. Different setups and specimens have been used by different researchers. Figure 3-1 shows some of the samples used to investigate interface shear transfer.

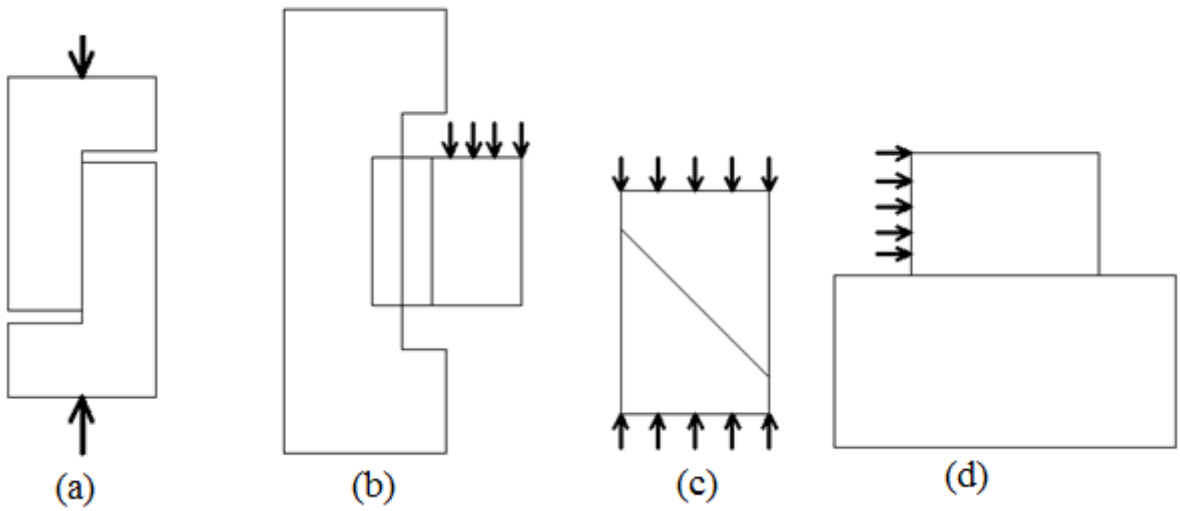



**Figure 3-1: Samples used to investigate interface shear transfer**

A push-off specimen shown in Figure 3-1(a) has been used by researchers from the past (mattock 1960, 1969, 1976; Walraven 1980) to recent studies (Julio et al. 2010, Figuiera et al. 2015; Rahal 2015, 2016). This specimen is advantageous because it allows the application of shear stress with minimum eccentricity. The other specimens are ideal to investigate the combination of shear with significant eccentricity ( Figure 3-1(b) and (d)) and compression

(Figure 3-1 (c)). But, a relative shear dominant behavior is obtained from the push-off specimen.

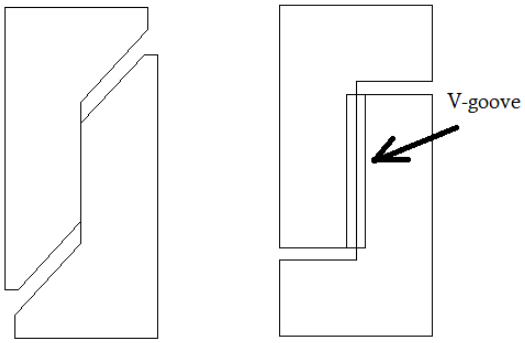



**Figure 3-2: Modifications to the push-off sample**

Different modifications have been made to the specimen for different purposes. Due to the geometrical shape of the specimen i.e. the gaps that exist between the "L" shaped concrete parts, the existence of small eccentricity and imperfections might cause failure on the top and bottom part of the push-off specimen before the interface fails. To prevent this type of failure push-off specimens like the one shown in Figure 3-2 has been used in different papers. V-groove might be introduced at the interface to reduce the surface area so that failure would be ensured to occur at the location of the interface. The sample has been used to study shear transfer on a pre-cracked interface, dowel action, fiber reinforced concrete, high strength concrete and so on (Mattock, 1969; Constantinescu, H., & Magureanu, C., 2011; Van Mier ). For the research at hand, a push-off specimen with V-grooves was found to be sufficient.

A preliminary FE model of the specimen without an interface was made on VecTor 3 to get a feel of the deformation pattern of the specimen. A tensile strain was observed on the top and side of the specimen (Figure 3-3), so an "L" shaped reinforcement was placed in the parts of the specimen to carry the tensile stress (Figure 3-5). Longitudinal bars parallel to the shear plane at the vicinity of the interface were not placed. This was done with the understanding that reinforcement in the critical zone near the interface contributes to the shear transfer mechanism (Thomas T.c.Hsu , S.T. Mau, and Bin Chen, 1987).

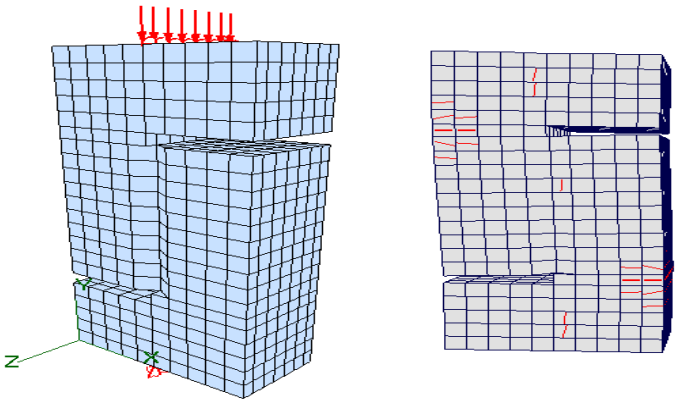


**Figure 3-3: Preliminary model of the Push-off specimen using VecTor3**

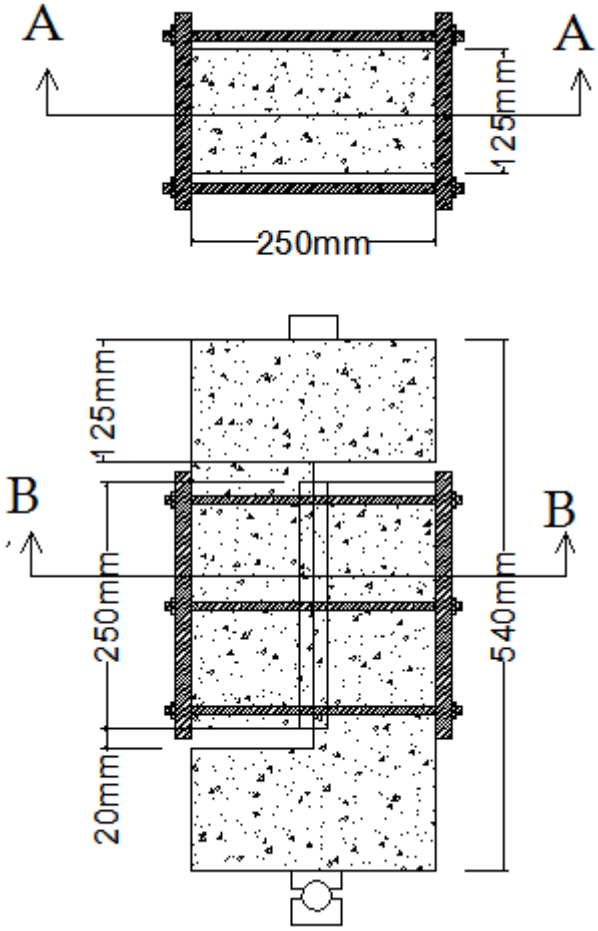



**Figure 3-4: Selected push-off specimen configuration**

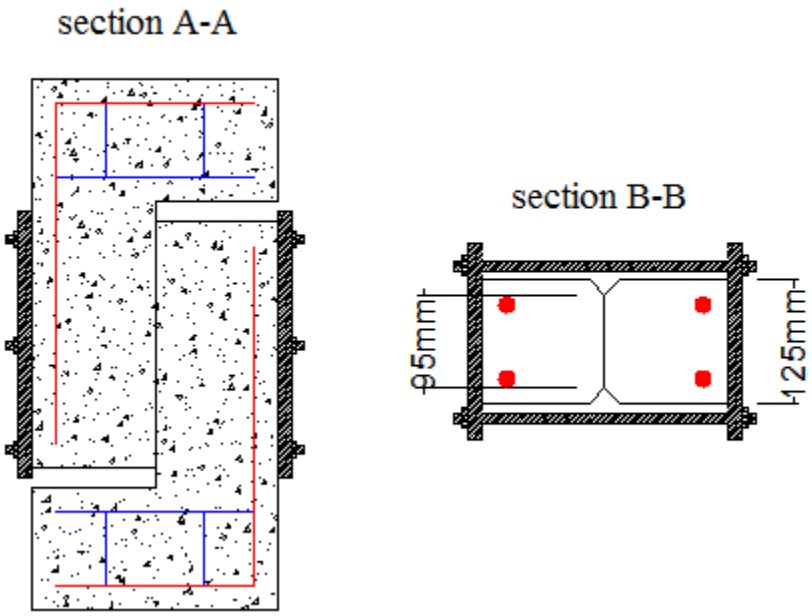



**Figure 3-5: Reinforcement layout of the selected push-off specimen**

## 3.2 Scope of the Experimental Program

In this study, Adhesive bonding was studied among the other shear transfer mechanisms. Dowel action and friction, which are mechanisms that are mobilized to a higher degree after de-bonding of the interface, are not covered in this study. Even though it has been reported that the contribution of dowel action before the interface de-bonds is small, dowel action was mechanically reduced in the experimental program intentionally. Two approaches have been used to minimize dowel action in literature. The first approach to diminish dowel action was by placing the reinforcement in a rubber sleeve inside the concrete (mattock, 1969). Another method was to put the reinforcement crossing the interface externally (Walraven, 1997). In the experimental program carried out, the latter approach was taken and the reinforcements were placed externally. The confining stress on the interface is indirectly measured through the strain gauges attached to the bars. It was also possible to reuse the external bars for other specimens since the yield strength of the reinforcement was not exceeded.

Three reinforcements were placed on the front and back side of the specimen; one at the bottom, one at the middle and one at the top of the interface. This was done with the understanding that the strain distribution over the interface will not be constant and strain reading on at least the three points will give an image of the deformation of the specimen

during testing. The bars crossing the interface were bolted on a thick plate attached to the concrete using an epoxy bonding agent called NITOBOND.

In this study two variables were considered; the amplitude of loading and the nature of the interface. The degradation nature of the interface between concrete cast at different times was studied in dry and moist environment for different levels of loading. Aside from the variables being investigated, other parameters were kept constant for all samples. The roughness of the interface, number of reinforcement crossing the interface, compressive strength of concrete, amount of initial confining stress applied on the interface, the time difference before casting the second part of the specimen, curing condition were all kept constant.

Three sets of specimens were considered. Three samples were cast on the first set. These samples were cast monolithically. Three samples were cast for the remaining two sets as well. The samples were cast to form a construction joint at the connection of the two parts. The second set of samples was tested in a dry condition while the third set of samples was tested in a moist condition. Three extra specimens were cast in order to perform a trial test to solidify test set up and instrumentation. For all specimens with an interface, the concrete parts were cast 24 hours apart.

One sample from each set of specimen was tested for monotonic loading to investigate the shear transfer mechanism in the three different conditions. Initially, a cyclic loading at high and medium load level was planned to be applied to simulate different scenarios of loading. But due to limitations of the experiment, this was not possible. First, since the load was applied manually using a hydraulic jack, large number cycles could not be applied. Second, with the limited number of specimens tested, it was not possible to accurately identify the percentage of load the cyclic load was applied to, so the raw data is presented.

Table 3.3 shows the specimen designation. The monolithically cast specimens are designated with three letters. The first letter “M” indicates that the specimens are monolithically cast. The second letter indicates whether the specimens were tested in the dry or wet condition. The third letter indicates the loading condition, whether it is monotonic or cyclic and for the cyclic loadings, the number shows the load level the cyclic load was applied to. For the other two sets of specimens, the first letter indicating the mode of casting is canceled out. For instance, specimen DC-75 is assigned to a specimen with an interface between concrete cast at different times tested in dry condition for cyclic loading up to a load of 75KN.

As mentioned above, three sets of specimens were prepared. The monotonic samples were done to serve as a control. The comparison between the monotonically cast samples and the samples with construction joints can tell us the nature of change of degradation when these weak interfaces are introduced on a structure. On the last set of samples, water exposure was investigated. Since construction joints could act as a conduit in the presence of water, it is important to investigate the effect of moisture on the degradation nature of adhesive bonding.

## 3.3 Material

### 3.3.1 Concrete:

Great care was taken in the fabrication of concrete to maintain a consistent mechanical property for all specimens. A mix proportion of 331.4Kg of cement, 916Kg of sand, 1056Kg of coarse aggregate and 97.5Kg of water per cubic meter of concrete after adjustment was used. Fairly similar concrete strength was achieved for all samples.

### 3.3.2 Cement

An ordinary Portland cement was used for all specimens.

### 3.3.3 Coarse Aggregate:

The coarse aggregate was washed before it was used since the silt content was high. The washed aggregated was sieved with a 25mm sieve and stored in a plastic bag as shown in Figure 3-6 until the time of mixing to maintain the moisture content. Physical tests of the aggregate were conducted and are presented in table 3.1.

**Table 3-1: Properties of coarse aggregate used**

| Material property | coarse Aggregate |
|---|---|
| Gradation | Well-graded |
| Unit weight | 1570kg/$m^3$ |
| Absorption | 1.54% |
| Specific gravity | 2.64% |
| Maximum aggregate size | 25mm |

### 3.3.4 Fine Aggregate:

The material used in the experiment was also washed to remove the excess silt. The final silt content was reduced to about 3%. The sand was stored in a plastic bag until the time of

mixing as done for the coarse aggregate to maintain the moisture content. The properties of sand used are presented in table 3.2.

**Table 3-2: Properties of fine aggregate used**

| Material property | fine Aggregate |
|---|---|
| Fineness modulus | 2.9 |
| Absorption | 0.8% |
| Silt content | 3% |



**Figure 3-6: Fine and coarse aggregates packed in a plastic bag**

### 3.3.5 Reinforcement

#### 3.3.5.1 Reinforcement Confining the Interface:

For the reinforcement bars passing through the interface externally, plain 10 bars were used. The stress-strain diagram for the same bars is presented in Figure 3-7.

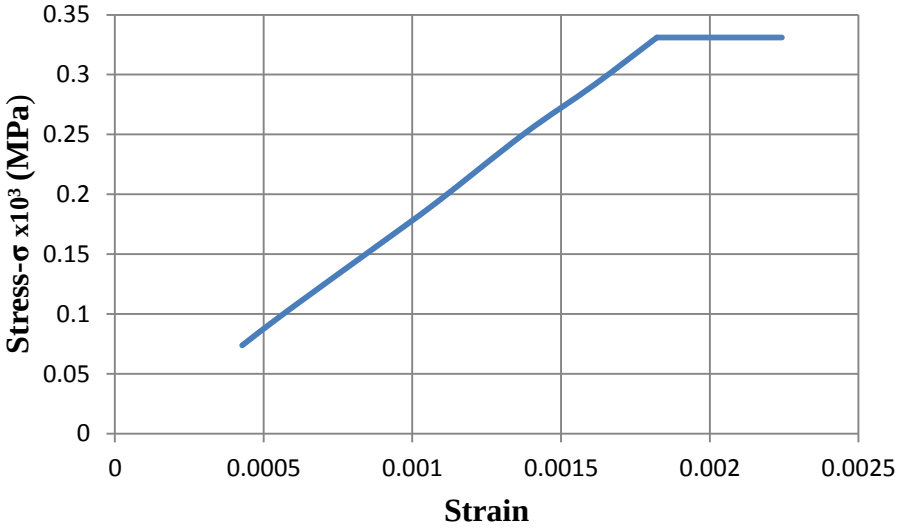



**Figure 3-7: Stress-strain diagram of reinforcement crossing the interface (Zerabruk, 2015)**

#### 3.3.5.2 Reinforcement inside Concrete:

The reinforcement placed inside each part of the concrete had a purpose of carrying tensile stress at locations indicated in Figure 3-3 and doesn't have any influence on the behavior of the interface. The bar had yield strength of 520MPa and an ultimate strength of 600MPa.

## 3.4 Specimen Preparation

The push-off specimens were cast in a metal formwork specially manufactured for this purpose (Figure 3-8). The formwork was first assembled and oiled to facilitate the removal of the metal plates. The prepared reinforcement was placed inside the formwork and appropriate spacing was provided.



**Figure 3-8: Metal Formwork**

The concrete constituents were mixed in a mixer shown in Figure 3-9. First, the coarse aggregate was placed in the mixer first followed by the cement and sand. Dry mixing of the materials was done for about one minute. After that, water is added and wet mix was done for one minute and a half. A similar procedure was done for all specimens. Slump test was done for each mix by a single person as a control to keep the consistency of the mix.



**Figure 3-9: Mixer machine**

The concrete was then placed in the formwork and compacted using a poker vibrator in an orientation indicated in Figure 3-10. For the specimens with a construction joint, only one half

of the specimen was cast and the other half was cast after 24 hours. The surface of the interface was left as vibrated without any roughening of the interface. This was a task assigned to a single person throughout the program since it is critical to maintain a similar surface roughness for all samples.

Four cubes were cast for each monolithically cast specimen and eight cubes were cast for each specimen with an interface to represent the compressive strength of the two constitutive parts. Due to the volume mixing capacity and small number of formwork available, it was not possible to cast all specimens in a set with a single mix. Table 3.3 shows the mix of each specimen in the composition column.



**Figure 3-10: Surface finish of the interface**

After the removal of the formwork, all the push-off specimens along with the cubes cast are placed in a water bath for curing. All specimens were kept soaked for the entire duration until the time of testing. After the specimens were taken out with their respective cube samples, they were left overnight to dry off. The next day, plates were attached with an epoxy resin called NITOBOND as shown in Figure 3-11 and left for three days to let the epoxy dry off. Loading plates were also attached using superglue.




**Figure 3-11: Plating of the push-off specimen**

**Table 3-3: Specimen designation and compressive strength**

| | **Push-off specimen designation** | **Loading condition** | **Composition** | **Cube compressive strength, MPa** | **Mean** | **COV** |
|---|---|---|---|---|---|---|
| **set 1: Monolithically cast specimens** | MD-M | Monotonic | Mix 1 | 50.2 | 53.11 | 3.9 |
| | | | | - | | |
| | | | | 54.03 | | |
| | | | | 55.06 | | |
| | MDC-110 | Dry condition 110KN cyclic | Mix 2 | 49.98 | 51.10 | 1.70 |
| | | | | 52.69 | | |
| | | | | 50.58 | | |
| | | | | 51.13 | | |
| | MDC-92 | Dry condition 92KN cyclic | Mix 3 | 49.27 | 49.39 | 0.99 |
| | | | | 49.73 | | |
| | | | | 49.82 | | |
| | | | | 48.75 | | |
| **set 2: Specimens under dry condition** | DM | Dry condition monotonic | BM12 | 49.03 | 48.43 | 1.01 |
| | | | | 48.07 | | |
| | | | | 48 | | |
| | | | | 48.63 | | |
| | | | TM14 | 49.23 | 48.63 | 1.25 |
| | | | | 49.08 | | |
| | | | | 48.08 | | |
| | | | | 48.13 | | |

| | | | | | | |
|---|---|---|---|---|---|---|
| | DC-75 | Dry condition 75KN cyclic | BM12 | 45.36 | 45.77 | 1.53 |
| | | | | 45.6 | | |
| | | | | 45.3 | | |
| | | | | 46.8 | | |
| | | | TM14 | 47.3 | 45.92 | 2.22 |
| | | | | 45.78 | | |
| | | | | 44.85 | | |
| | | | | 45.73 | | |
| | DC-70 | Dry condition 70KN cyclic | BM13 | 41.35 | 40.95 | 4.79 |
| | | | | 41.35 | | |
| | | | | 42.88 | | |
| | | | | 38.21 | | |
| | | | TM15 | - | 54.27 | 3.26 |
| | | | | 53.02 | | |
| | | | | 55.52 | | |
| | | | | - | | |
| **set 2: Specimens under moist condition** | MM | Moist condition monotonic | BM4 | 53.43 | 50.51 | 5.63 |
| | | | | 46.64 | | |
| | | | | 51.38 | | |
| | | | | 50.57 | | |
| | | | TM6 | 49.05 | 51.90 | 4.09 |
| | | | | 51.53 | | |
| | | | | 53.38 | | |
| | | | | 53.65 | | |
| | MC-82 | Moist condition 82KN cyclic | BM4 | 48.87 | 51.87 | 6.02 |
| | | | | 52.26 | | |
| | | | | 50.28 | | |
| | | | | 56.06 | | |
| | | | TM6 | 54.19 | 52.48 | 3.09 |
| | | | | 52.28 | | |
| | | | | 50.96 | | |
| | | | | - | | |
| | MC-60 | Moist condition 60KN | BM9 | 43.2 | 45.99 | 6.26 |
| | | | | 48.95 | | |
| | | | | 45.83 | | |
| | | | | - | | |
| | | | TM11 | 49.19 | 49.83 | 1.38 |
| | | | | 50.56 | | |
| | | | | 49.73 | | |
| | | | | - | | |

## 3.5 Test Setup and Instrumentation

A trial test was necessary to come up with an acceptable test set up and instrumentation to study the one-directional cyclic loading. Three push-off samples were cast for a trial test. All specimens were cast forming a construction joint on their interface by casting the two parts of concrete 24 hours apart. Initially, a universal compression machine shown in Figure 3-12 was used. One specimen was loaded monotonically and the other two were loaded with a one-directional cyclic shear loading.

As for instrumentation, three transducers were placed on each face of the specimen, two measuring transverse opening on the top and bottom part of the interface and one measuring slip as shown in Figure 3-12. Strain gauges were placed on the external steel bars to measure the confining stress. A load cell indicated in Figure 3-12 was used to measure the load being applied. The load cell and the transducers were not compatible on a single data logger so two separate data loggers were used to read the load and displacement. The recording on both loggers was started at the same time to match the two readings.

A small initial confining stress was applied by tightening the bolts on the confining bars. A constant confining strain of 100με was initially provided for all specimens throughout the program.

Roller support was provided at the top and bottom of the specimen for the trial set up. This was done to eliminate restraint on the specimen from deforming horizontally. The round bar was placed in between half cut loading plates.



**Figure 3-12: Trial test set up and instrumentation**

According to the result, the set up used had the following drawbacks.

- It was not possible to control the load rate at a needed level. The load applied fluctuated on its own as shown in Figure 3-13.
- The load versus slip diagram was also not realistic. Aside from the fact that the load and displacement were measured with different data loggers, the accuracy of the transducers could not capture the deformation in a clear manner.
- Using roller support at the top and bottom of the specimen made the system unstable. Small eccentricity would make the specimen fall.

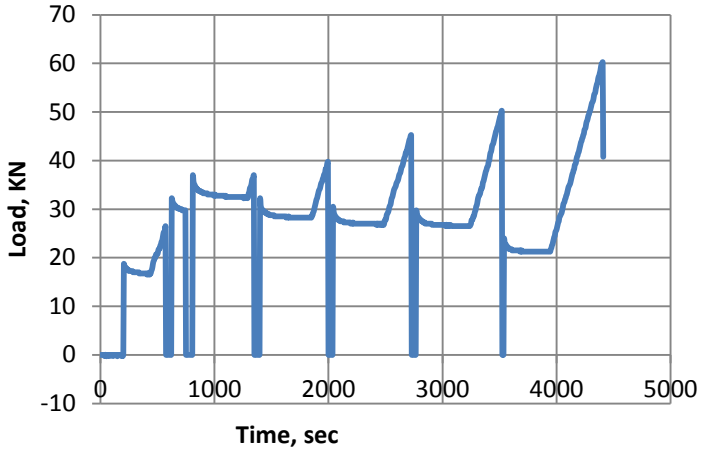



**Figure 3-13: Load rate applied using an automatic compression machine**

To tackle the load rate problem, it was decided to use a hydraulic jack and apply the load manually. Styrofoam was placed at the sides of the push-off specimen to keep it from losing its position at the time of unloading (Figure 3-14). But, later during testing, it was observed that the hydraulic jack itself kept the specimen in place during unloading but the Styrofoam was placed for all tests as a precautionary measure.

A different set of transducers which were compatible with the data logger of the load cell were tried out. The transducers were attached to the concrete surface using super glue. The transducer was attached to one part of the specimen while a plate attached to the other part which comes in contact with the transducer allowing the measurement of the relative displacement of the two parts. As for the support condition, after considering different options, the roller at the top of the specimen was removed and replaced with a flat plate to ensure the stability of the specimen (Figure 3-14).



**Figure 3-14: Second trial test set up and instrumentation**

With the new set up used, it was possible to control the load rate and apply a one-directional cyclic load (Figure 3-15). Even though the process is laborious, it was used for the remaining specimens. The support condition also proved to be stable while still not restraining the specimen horizontally.

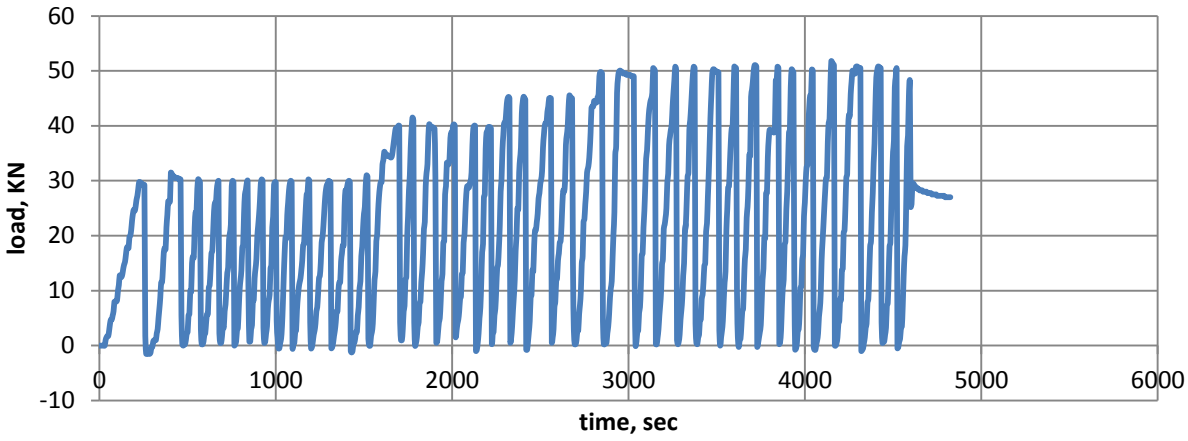



**Figure 3-15: Load rate achieved using a manually operated hydraulic jack**

Similarly to the transducers used in the first set up, the new transducers used could not capture the displacement of the specimen with a good accuracy as shown in figure 3.16. To capture the small displacement of the interface of the push-off specimen was a challenge in the experiment.

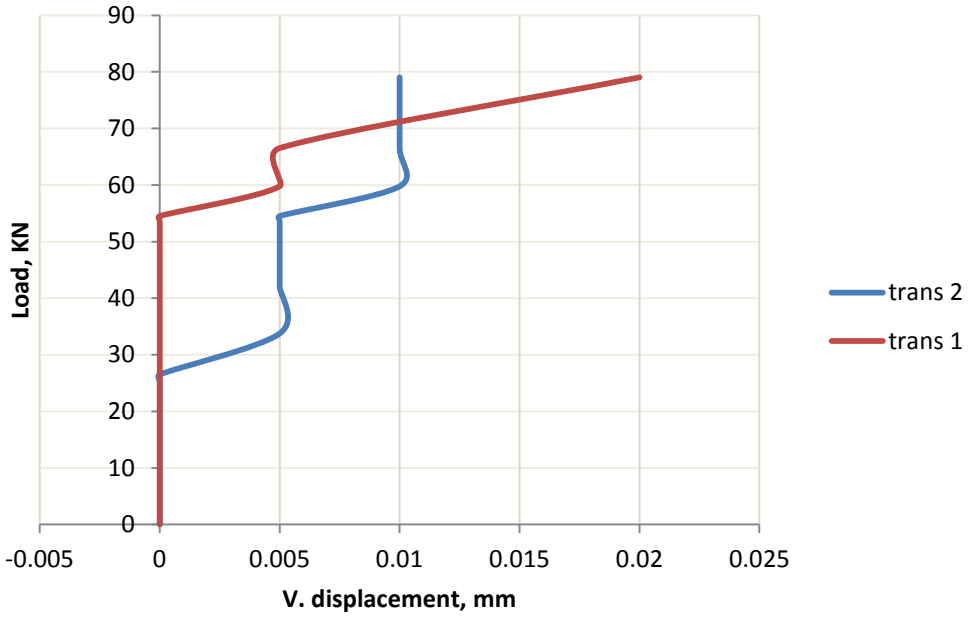



**Figure 3-16: Displacement versus load with a displacement measured by transducers**

It would be more convenient to represent this displacement in terms of strain since the interface before de-bonding is continuum. It is also possible to measure strain using concrete strain gauges with an acceptable accuracy since the strain at the interface is within the range of sensitivity of the strain gauges. By utilizing strain transformation concept, it is also possible to calculate shear strain and axial strain in any orientation if axial strain in three directions ($\varepsilon_x$, $\varepsilon_y$ and $\varepsilon_{45}$) is measured as shown in Equation 3-1 and Equation 3-2.

$$\varepsilon_\theta = \varepsilon_x \cos^2\theta + \varepsilon_y \sin^2\theta + \gamma_{xy} \sin\theta\cos\theta \qquad \textbf{Equation 3-1}$$

Substituting $45^o$ for θ, Equation 3-1 can be rearranged to calculate the shear strain as:

$$\gamma_{xy} = 2\varepsilon_{45} - \varepsilon_x - \varepsilon_y \qquad \textbf{Equation 3-2}$$

Before applying this technique to the push-off specimen, a trial measurement was done on a cube sample. Two major challenges were faced undertaking this method: the first one was the difficulty to acquire a rosette strain gauge and the second was the existence of a grove at the interface which was made to ensure failure at the interface.

Rosette strain gauges are manufactured to measure strain in two perpendicular directions and a third direction in between the two axes as shown in Figure 3-17. Since only single strain gauges were available, it was decided to attach three different strain gauges in three different directions in a way that they don't interfere with each other. As for the grove, stucco was to be placed to fill the gap where the strain gauge was to be attached. After placing the stucco in place, a plastic was super glued to the interface in order to attach the strain gauge. The trial cube sample is shown in Figure 3-18.

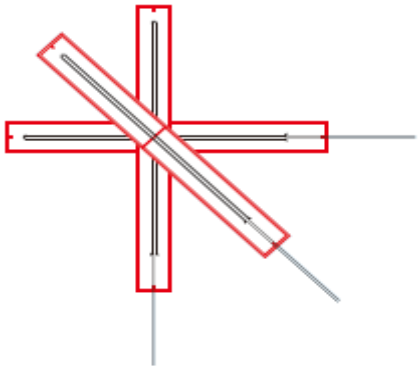


**Figure 3-17: Rosette strain gauge**

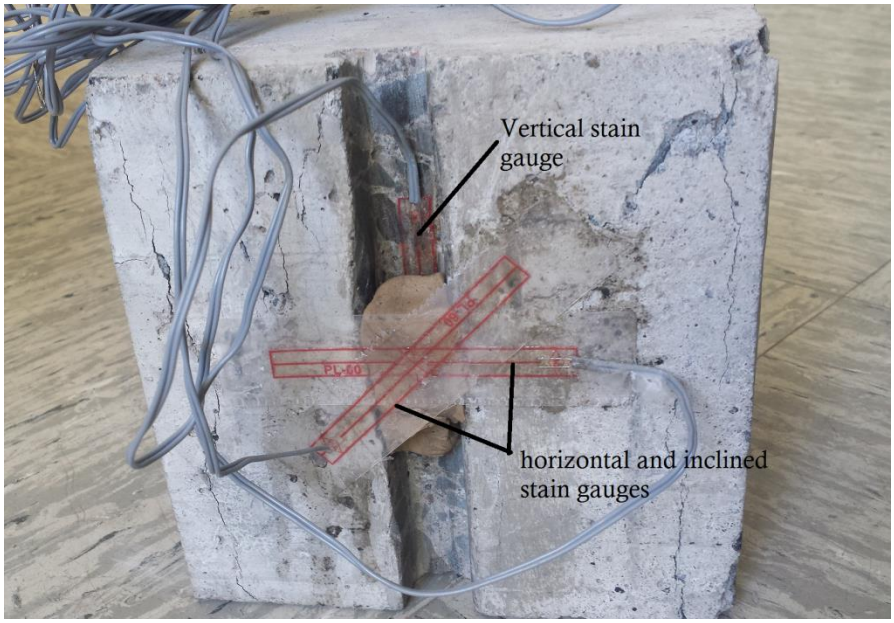



**Figure 3-18: Application of strain gauges on a grooved cube sample**

A vertical strain gauge was attached inside the grove to measure strain in the vertical direction. The horizontal and inclined strain gauges where placed on stucco that filled the grove. First, the cube was loaded using a manual jack system. A load cell was used to measure the load applied as shown in Figure 3-. Using the three strain measurements the

shear strain was calculated using simple strain transformation equation. Figure 3-21 shows the obtained result. As it can be seen, the strain in the direction of loading, εy, showed an almost linear increase of compressive strain as would be expected, But strain in the transverse direction was compression as well at the beginning of the test and gradually became a tensile strain. This inconsistency was probably caused by lack of uniform load application on the cube since loading jack was used.



**Figure 3-20: Load by a jack**



**Figure 3-19: Load by a compression machine**

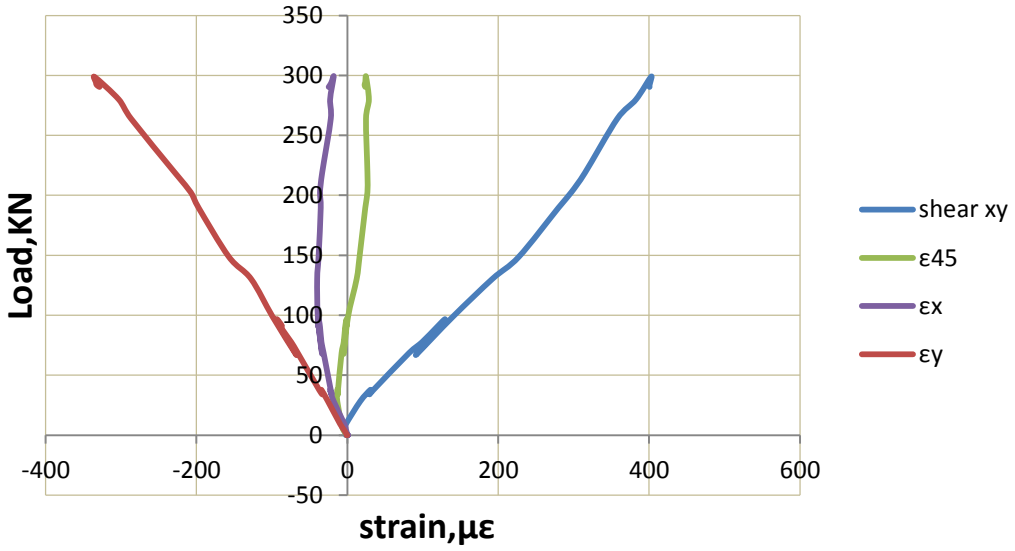



**Figure 3-21: Strain versus load diagram of a cube specimen for the load applied using jack**

Next, the cube was tested in a compression machine as shown in Figure 3-19. Figure 3-23 shows the result of the strain gauges up to maximum strain. As expected, the longitudinal and

transverse strain readings where compressive and tensile strain respectively. The strain measurement at an angle of 45$^{o}$ was in between the two orientations. The Poisson's ratio was computed using Equation 3-3 from the data and was between 0.16 and 0.25 before significant cracks occurred (Figure 3-22). This can confirm the reliability of the data.

$$\nu = \frac{Lateral\ strain\ (\varepsilon_x)}{Axial\ strain\ (\varepsilon_y)} \qquad \textbf{Equation 3-3}$$

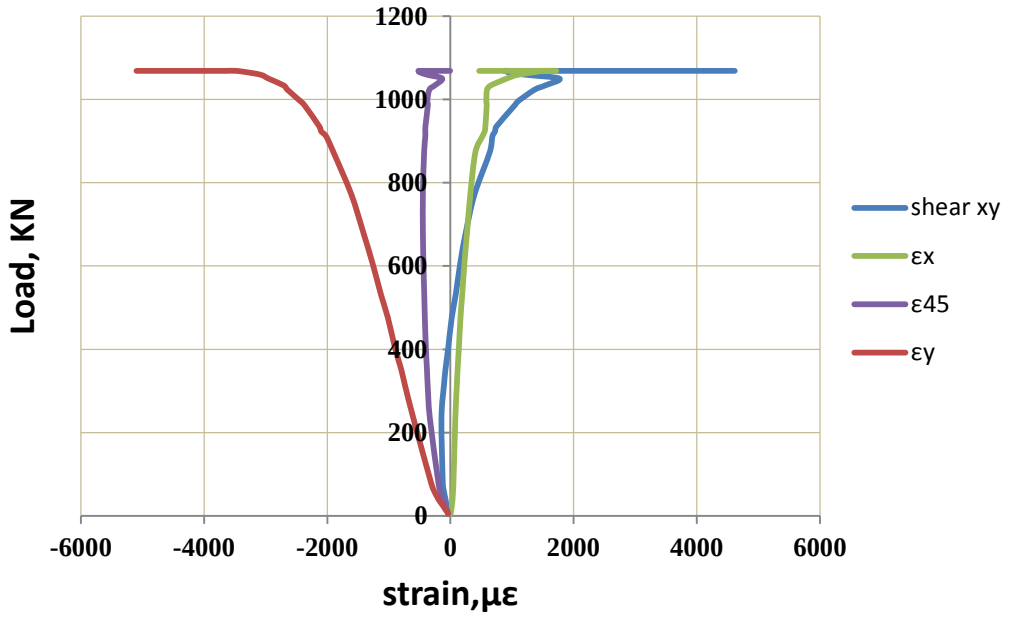



**Figure 3-23: Strain versus load graph for a cube specimen using a compression machine**

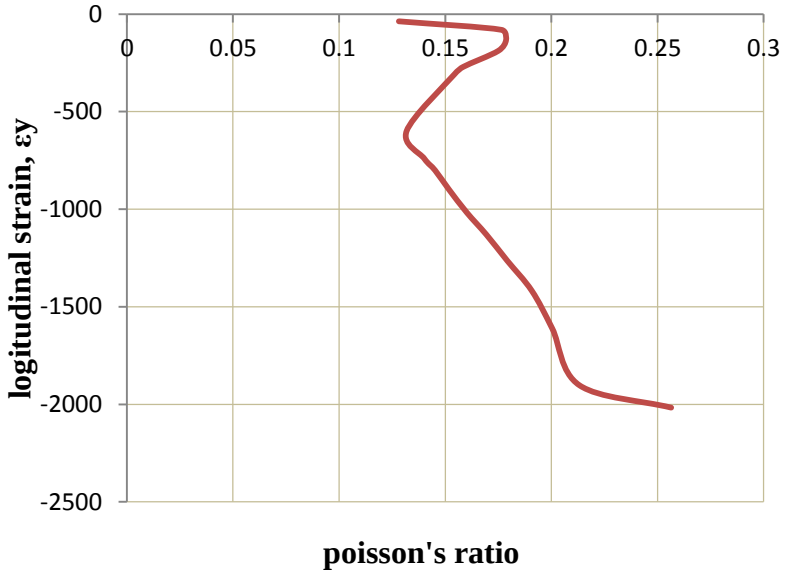



**Figure 3-22: Poisson's ratio**

Using the three readings, the shear strain was calculated. It is also possible to construct Mohr's circle for each load stage as shown in Figure 3-24.

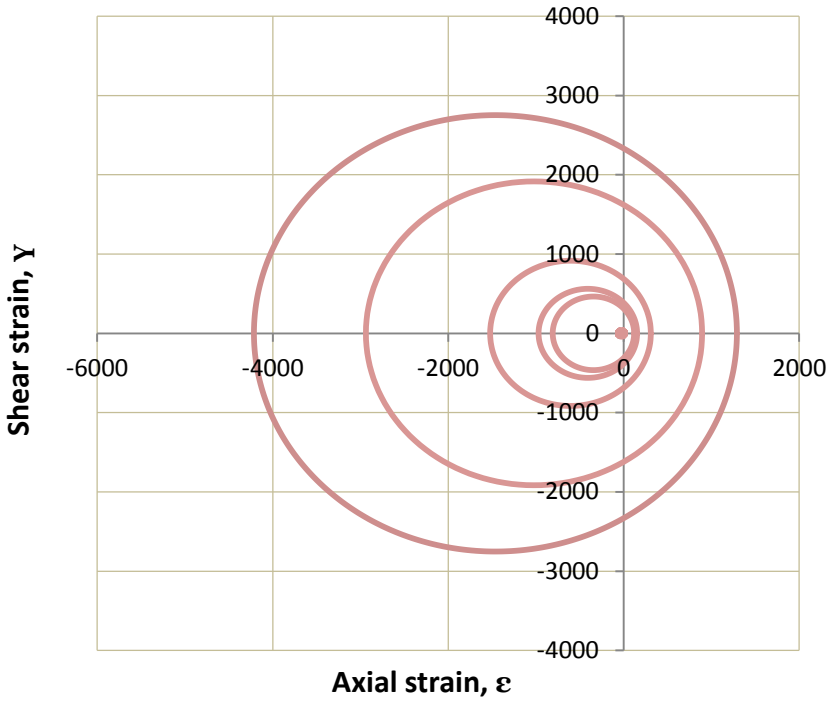



**Figure 3-24: Mohr's circle for selected points**

In general, from the trail test, we can conclude that:

- It is possible to measure the shear strain with the method employed.
- The strain gauge readings are very sensitive so great care should be taken to apply the load as uniform as possible.

So finally, the set up shown in Figure 3-25 was used for the push-off specimens tested under dry condition. The set of concrete strain gauges were placed in the middle of the interface at both faces. It would have been more convenient to attach the set of strain gauges at least at two points on each side of the interface to get a more accurate deformation of the specimen but due to lack of instruments, it was not possible to do so.




**Figure 3-25: Final test set up and instrumentation for specimens loaded in dry condition**

To test the interface in a moist condition, a custom tanker was manufactured. The tanker was constructed of metal sheet except for one face of the tanker which was made to be a transparent glass to monitor the specimen while testing. The load cell was placed under the tanker to measure the load being applied. Special care had to be made to place the tanker at the center of the load cell to avoid overturning of the whole set up (Figure 3-26).

The bottom plate on which the round roller bars rest on was welded to the bottom of the tanker to avoid slipping of the specimen in water. Another challenge was to keep the Styrofoam in place when the water was filled. The Styrofoam was pushed up by the buoyancy force of the water. Restraining plates were placed outside the tanker to keep the Styrofoam in place. Another concern was the functionality of the strain gauges under water. Even though the wires of the strain gauges are coated, gasket maker was placed on the wires to keep water from entering and creating a short circuit.

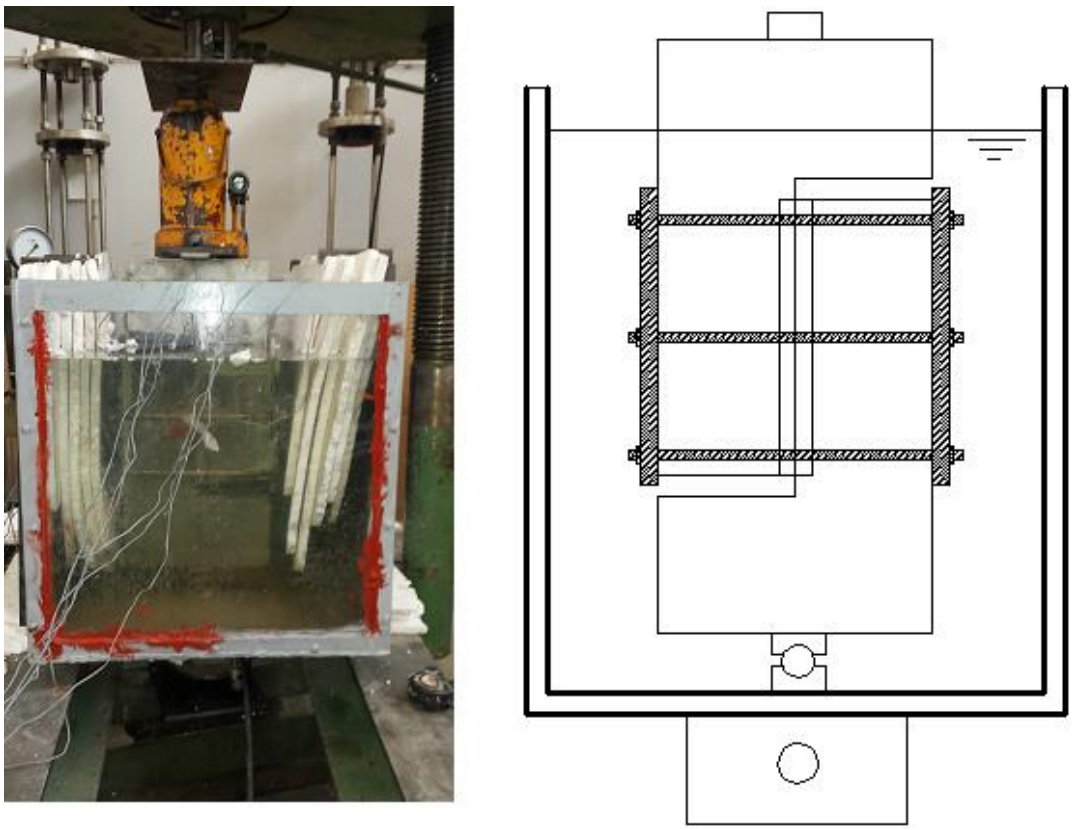


**Figure 3-26: Test set up for specimens tested in moist condition**

# 4 EXPERIMENTAL RESULTS AND DISCUSSION

In this section, the experimental results accompanied by the discussion are presented. Since it was quite difficult to tell at what percentage the cyclic loads where being done with the limited number of specimens tested, a specific percentage is not given to each specimen. The designation of the specimens is provided in terms of the maximum load the cyclic load was applied to. However, the load and strain level of each specimen at the first cycle is presented as a percentage of the specimen tested monotonically at a dry condition in Table 4-2. This sample was selected because all cyclically loaded specimens showed a similar deformation pattern with the specimen on the first cycle of loading.

Due to faulty deformation measurement during the test of the specimens cast monolithically, only the peak load and number of cycle is presented. Observation during the test of each specimen in the dry and moist condition is discussed. And finally, the comparative discussion is given between the three set of samples.

## 4.1 Results of Monolithically Cast Specimens

Three specimens without an interface were tested for different loading condition. The sample tested monotonically failed at 131KN. Failure occurred at the notch of the specimen. The failure surface was rough due to the existence of aggregate at the interface. Crack propagated around the aggregate when the surrounding paste was weaker than the aggregate, otherwise the crack cut through the aggregate (Figure 4-1).

The second specimen was tested for cyclic loading up to the load of 110KN. This is 84% of the full capacity of the specimen tested for monotonic loading. However, it is not possible to be sure of the percentage of loading considering the stochastic behavior of concrete. The specimen failed after only 4 cycles.

Considering the small number of cycle to failure for the second specimen, a load at 70% of the capacity of the specimen tested monotonically was applied. The specimen withstood a thousand cycle of loading without de-bonding. After that, a monotonic load was applied to investigate the residual shear strength of the specimen. Unpredictably, the specimen de-bonded at 148KN, which was greater than the capacity of the sample tested for monotonic loading condition. While this increase in strength might be attributed to the stochastic behavior of concrete, other factors could be cited as a possible cause. One reason could be the

consolidation effect of the load on the concrete. When a concrete element is under compression, at the initial stages of loading, a stiffening behavior might be encountered due to the closure of micro-pores of concrete. This behavior has been reported as a possible cause of strength enhancement under fatigue loading in uniaxial compression of concrete (Isojeh, B., 2007). The second speculation is the mobilization of internal friction due to the micro-cracks formed during the cyclic loading stage. Figure 4-2 shows the average confining stress versus load applied of the monotonically loaded specimen, the specimen that was tested monotonically after applying a 1000 cycle and the final cycle of the specimen that failed at the fourth cycle. The confining stress is calculated from the strain measurements taken on the confining bars. The monotonically loaded specimen de-bonds at the point where the graph drops and gradually regains its strength due to the mobilization of friction. After this re-strengthening, the specimen reaches a second peak strength and stabilizes. On the other hand, the specimen that had been cyclically loaded stiffness before the interface de-bonds and after de-bonding, re-strengthening is not observed. This could be an indication of friction being mobilized before total de-bonding of the interface.

The debris of the interface after completing the test was analyzed. As expected the specimen that passed through a high number of cycles had a larger quantity of debris in general and the debris was finer in size as well (Figure 4-1).

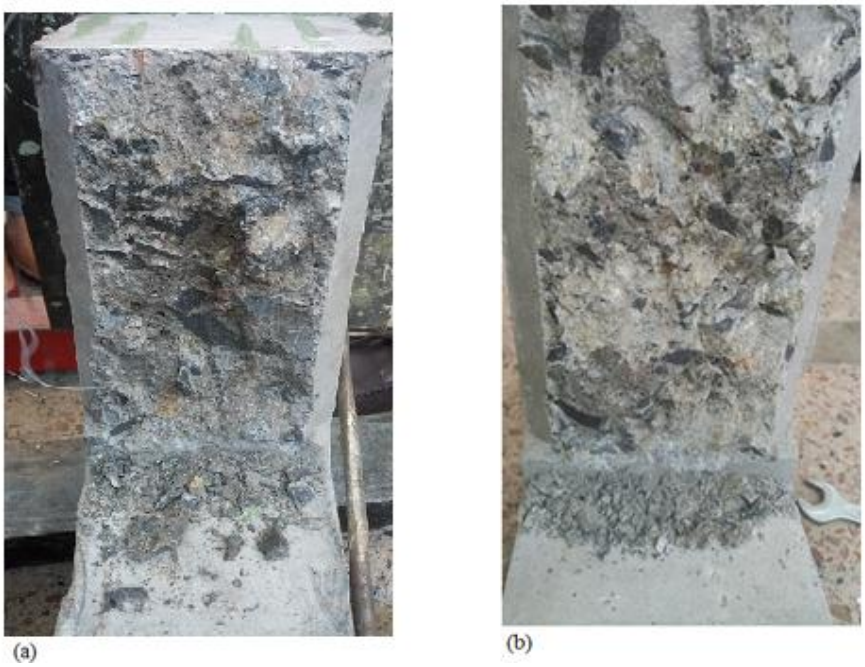



**Figure 4-1: Cracked surface of monolithically cast specimens (a) monotonically loaded specimen; (b) cyclically loaded specimen**

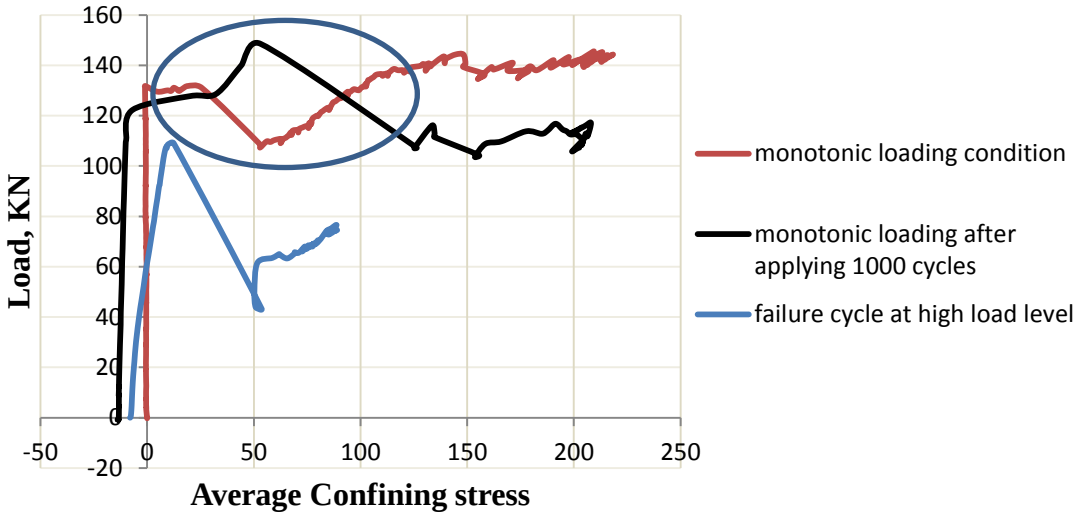



**Figure 4-2 Average confining stress to load applied of monolithically cast specimens at failure cycle**

## 4.2 Results of Specimens with the Interface in Dry Condition

### 4.2.1 Specimen DM

The test on the specimen for monotonic loading with the proposed instrumentation setup showed an average deformation as shown in Figure 4-4 (a). As expected a compressive strain was observed vertically (εy) while a dominant tensile strain was recorded horizontally (εx). The Poisson's ratio was significantly higher than that of the cube sample tested for the trial due to the geometrical configuration of the push-off specimen. The strain measurement at 45$^{o}$ laid in between the two strain readings deviating more to the dominant one. The orientations and symbols used in the charts is shown in Figure 4-3.

At the instant of total de-bonding of the interface, the horizontal strain gauges detached from the specimen which explains why the horizontal strain readings show a compressive strain after de-bonding. Due to this, it was not possible to calculate the shear strain after de-bonding. In addition, it can be seen that the vertical strain readings reduce at the point of de-bonding. The mobilization of slip at the interface relieves stress at the adjacent concrete. After the concrete has totally de-bonded, the vertical strain reading cannot be used to calculate shear strain since the crack creates discontinuity and the vertical strain at the interface cannot be captured with these readings. Slip measurement with a transducer after

de-bonding is more plausible. For this reason, the post-peak diagram of the shear strain is not shown for the all the specimens.

The strain readings at the front and back side of the specimen are not identical. All three strain readings are higher in the front side of the specimen. Variation in the vertical compressive reading of the interface at the two sides indicates a twisting motion at the interface while a variation of the horizontal readings indicates a larger "opening" at one side of the interface. This phenomenon may be attributed to three different reasons:

- Roughness of the interface or protruded aggregates at the interface.
- Imperfect distribution of load over the loading plate
- Small variation during tightening of the bolts of the confining bars.

The horizontal strain reading at the back side of the specimen seemed to be decreasing after applying an average shear strain of 3MPa at which point the horizontal strain accompanied with the shear strain of the front side began to increase at a higher rate (Figure 4-4(b)). This phenomenon indicates that the damage is being localized at one side of the specimen.

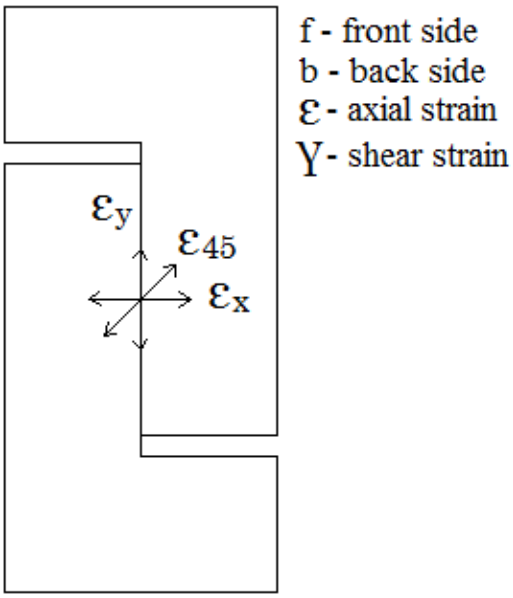
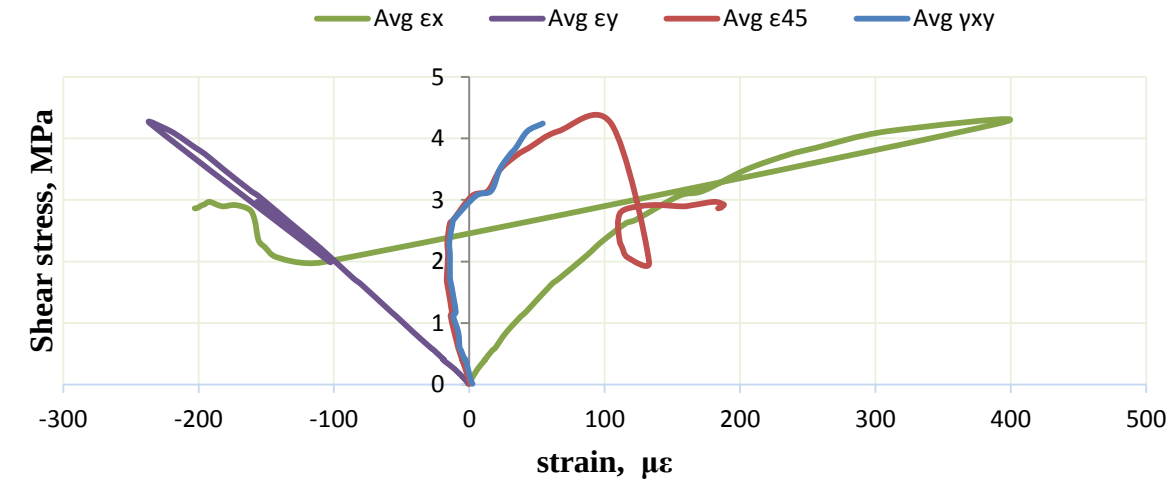
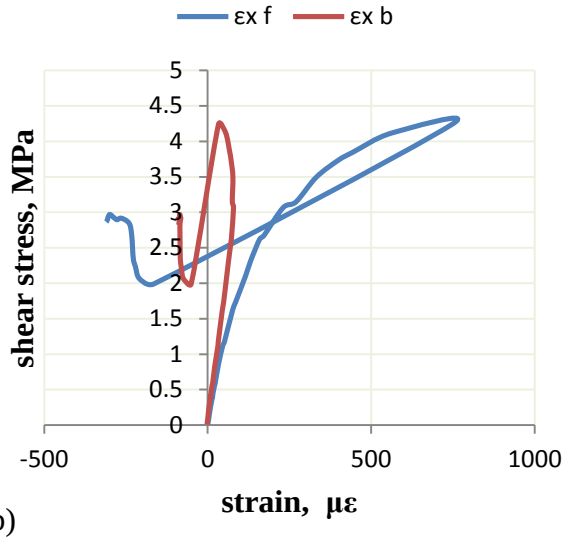


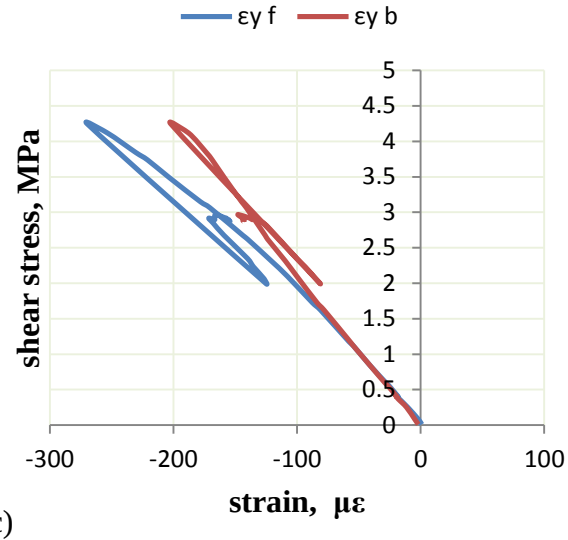

**Figure 4-3: Orientations and symbols used in the charts**



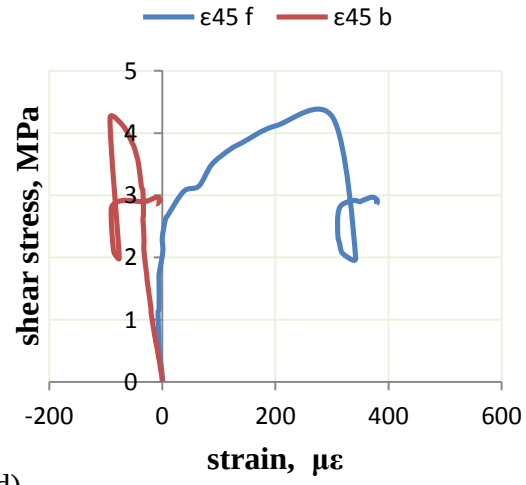

(a)



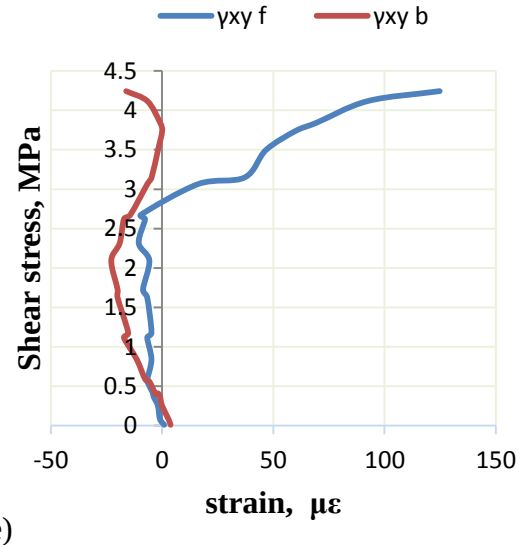

(b)




(c)




(d)




(e)

**Figure 4-4: Average shear stress to strain curve of specimen DM (a) all average strain of the interface; (b) horizontal strain at the front and back side; (c) Vertical strain at the front and back side; (d) strain at an angle of 45$^{o}$ at the front and back side; (e) shear strain at the front and back side up to peak stress**

The shear strain calculated from the vertical, horizontal and inclined strain readings shows a negative deformation at the beginning of loading and eventually attains a positive deformation to the point of de-bonding (Figure 4-4(e)). The diagrammatical representation of the positive and negative shear deformation is shown in Figure 4-5. Although it may seem unrealistic that the specimen attains a positive shear deformation with the given loading condition, two possible reasons can be mentioned. First, since it is difficult to avoid eccentricity completely, such type of deformation might be caused (Figure 4-6). But at the point of de-bonding, it is inevitable that the graph attains a large negative strain. Second, the existence of substantial tension and compression stress at the interface could have affected the deformation mode of the interface. However, it is important to note this occurs at a very small strain as compared to the de-bonding strain.

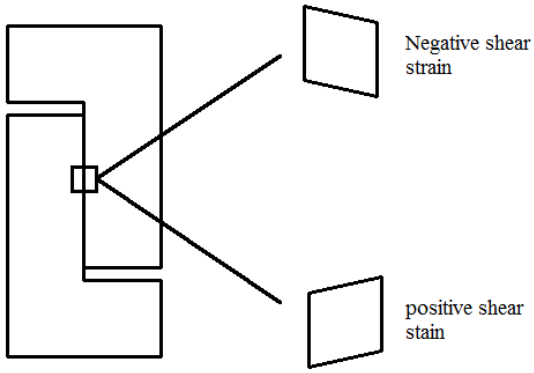



**Figure 4-5: Orientation of shear deformation**

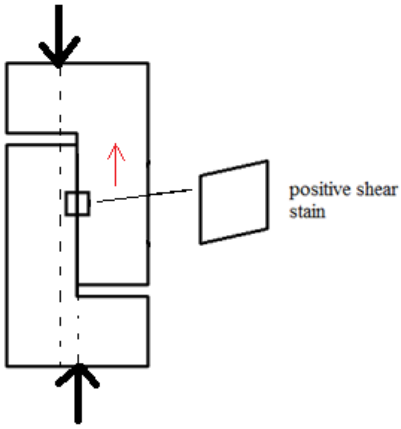



**Figure 4-6: Possible eccentric loading**

### 4.2.2 Specimen DC-75

A one-directional cyclic load at 75KN was applied to the specimen. In terms of the shear strain and horizontal tensile strain, this load was at 75% of the monotonically loaded sample. The deformation of the specimen at the first cycle was nearly identical to the one tested monotonically except the major deformation was localized at the back side of the specimen. The specimen failed after applying 994 cycles of loading over a period of four days.

The horizontal strain on the back side showed the largest deformation rate during the cyclic loading of the specimen as compared to the other readings. Figure 4-7 (b) shows a typical degradation curve, with a high rate at the first cycles and eventually coming to a reduced and an approximate linear degradation rate. (Isojeh, B., 2007) During this stage, the strain at the front side remained constant indicating that degradation was localized to one side of the push off sample. After about 540 cycles, a rapid increase in peak horizontal strain was observed. The side that was in compression horizontally increased in degradation rate and finally became similar to the other side. This is an implication of crack propagation from one side of the specimen to the other side through the interface. At the final cycles of the test, unstable cracks were formed. When the peak load was reached, the crack propagated without an increase in load, unlike the behavior observed at earlier cycles of loading.

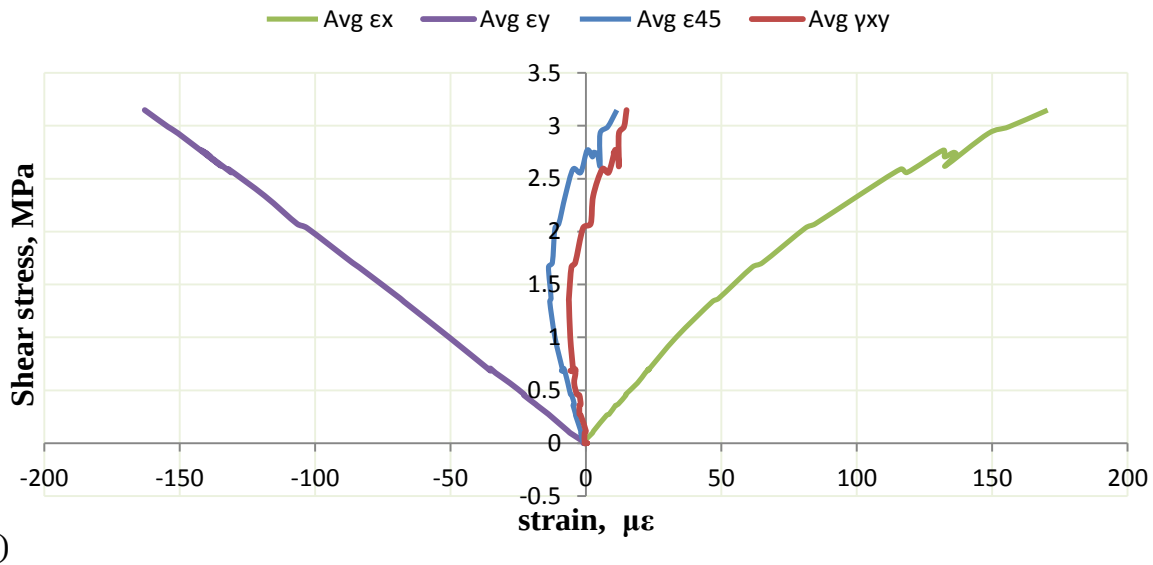
Significant degradation was not observed in the vertical strain. This is probably due to the fact that compressive stress is not dominant at the interface due to the gaps between the top and bottom parts of the specimen which creates a discontinuity to the stress trajectory. In addition, at higher cycles of loading, microcracks start to form at the interface, creating a discontinuous region and relieving stress at the place where the vertical strain gauges are attached.

The shear strain at the front side of the specimen remained positive for the first few cycles and after about the 500th cycle both sides showed a negative shear strain, which is an indication of damage propagating from one side of the specimen to the other. The degradation rate was small at the beginning of the cycles and increased drastically after the horizontal strain at the front side started increasing.

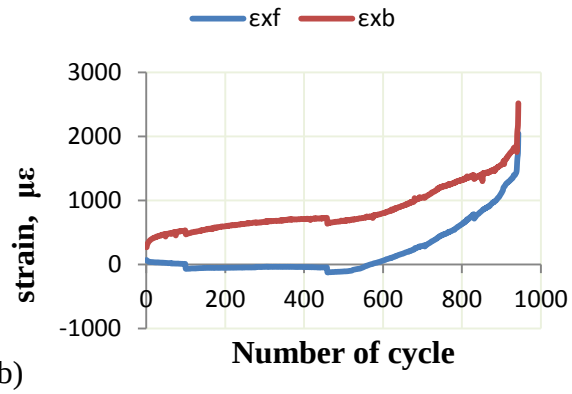
Figure 4-8 shows the evolution of average shear strain with average shear stress at the interface. The graph shows clear shear stiffness degradation as the number of cycles increase.

For the first few cycles of loading, the shear strain remained in the positive range. As the number of cycles was increased the strain attained a negative value which means the specimen is deforming in a manner shown in Figure 4-5. This indicates that with the damage evolution, shear deformation becomes pronounced.

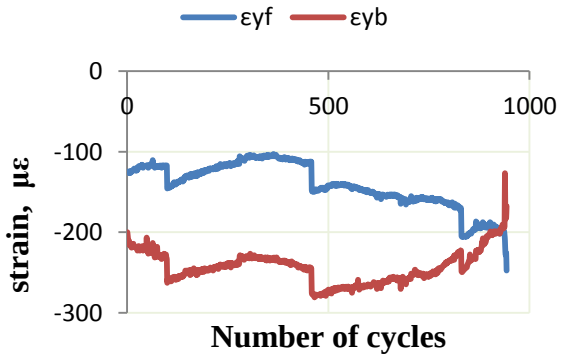
As the number of cycles progressed, visible crack was formed at the interface. The crack closed and opened during the unloading and loading process respectively. At the final cycles of loading, unstable cracks were formed. The shear strain increased at a constant load at the peak as shown in Figure 4-8. After the formation of unstable cracks, the specimen only lasted a few cycles and de-bonding occurred at the 994th cycle.




(a)




(b)




(c)

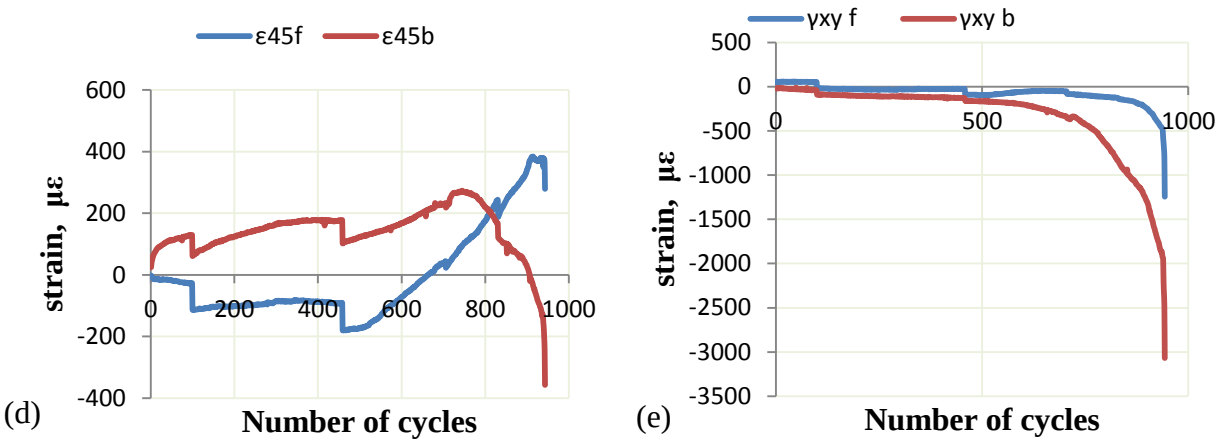



**Figure 4-7: Result of specimen DC-75 (a) Average strain of the interface to average shear stress; (b) Evolution of horizontal strain at the front and back side with number of cycle; (c) Evolution of Vertical strain at the front and back side with number of cycle; (d) Evolution of strain at 45$^{o}$ at the front and back side with number of cycle; (e) Evolution of shear strain at the front and back side with number of cycle**

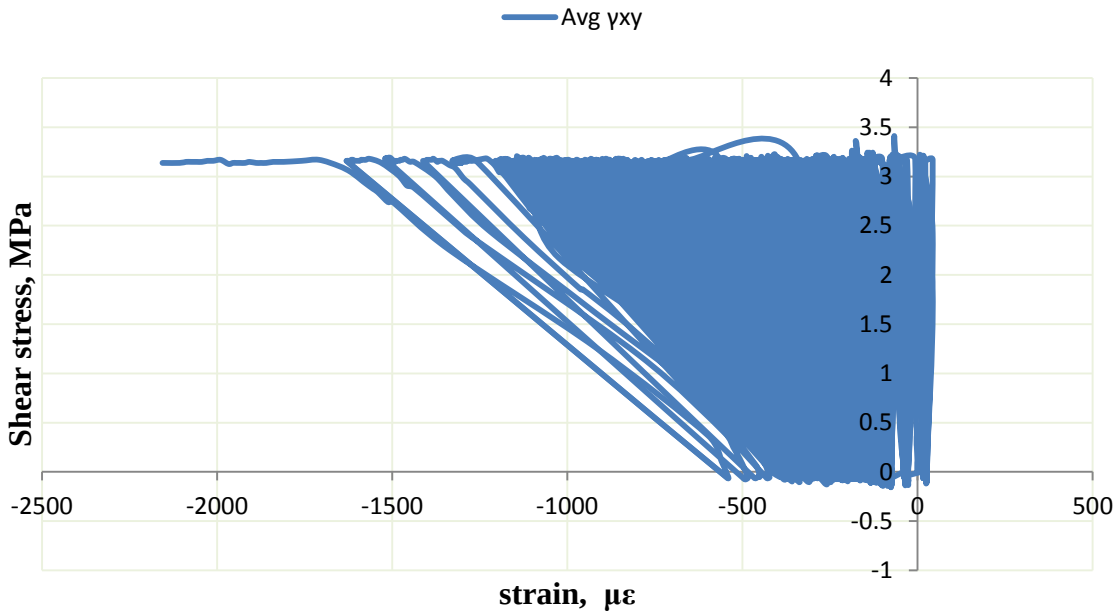



**Figure 4-8: Shear stress – strain curve of specimen DC-75**

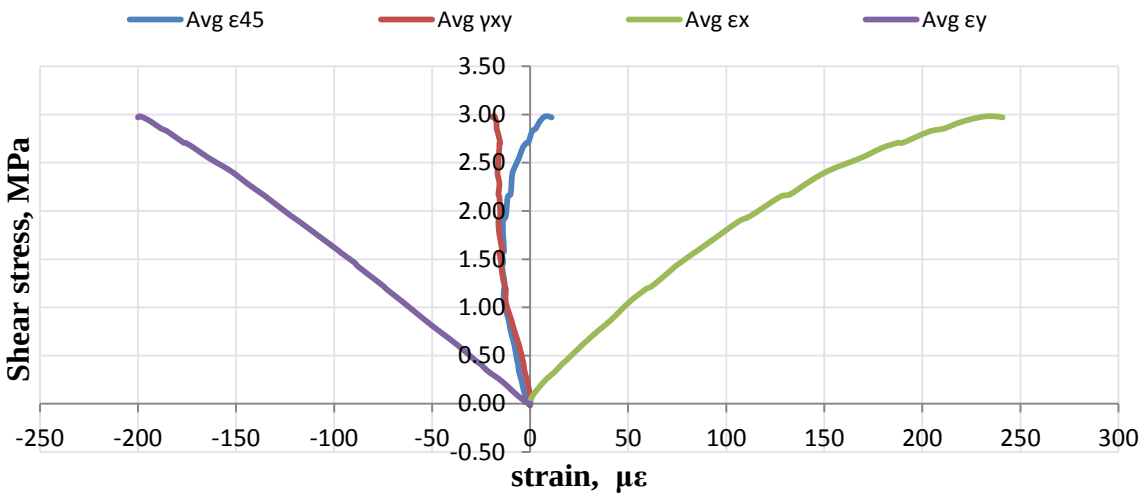
### 4.2.3 Specimen DC-70

A one-directional cyclic load at 70KN was applied to the specimen. The shear and the horizontal strain were at -80% and 85.5% of the monotonically loaded specimen respectively. The minus sign indicates an inversed deformation shape. Initially, it was decided on the 70KN during testing to attain 85% the horizontal tensile strain of the monotonically loaded specimen.

The deformation pattern was similar to the first two samples. Strain readings at the front side were greater than that of the back side because there was a twist at the interface due to reasons discussed on section 4.2.1 Even though the initial strain was high at the interface, the specimen eventually stabilized and sustained through 1000 cycles (Figure 4-9). Since the load was applied manually, it was not possible to go further so a monotonic load was applied to investigate the residual shear strength of the interface. The specimen then failed at 88KN.

All strain readings showed a rapid increase in rate for the first few cycles and eventually stabilized. The vertical strain and the strain at $45^{o}$ had a higher degree of stabilization while the horizontal and shear strains increased at a higher rate. The average shear strain versus average shear stress shows clear shear stiffness degradation as the number of cycles increased (Figure 4-10).

(a)



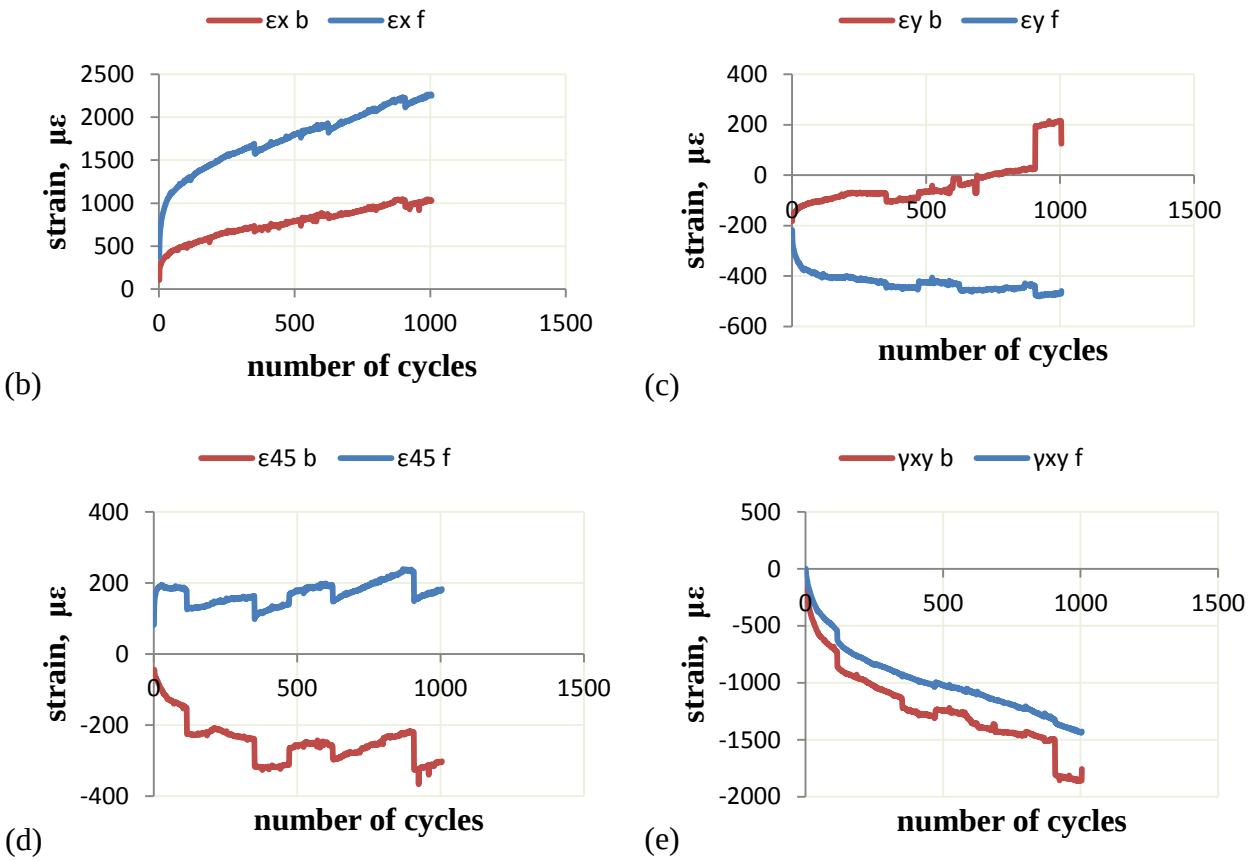



**Figure 4-9: Result of specimen DC-70 (a) Average strain of the interface to average shear stress; (b) Evolution of horizontal strain at the front and back side with number of cycle; (c) Evolution of Vertical strain at the front and back side with number of cycle; (d) Evolution of strain at 45$^{o}$ at the front and back side with number of cycle; (e) Evolution of shear strain at the front and back side with number of cycle**

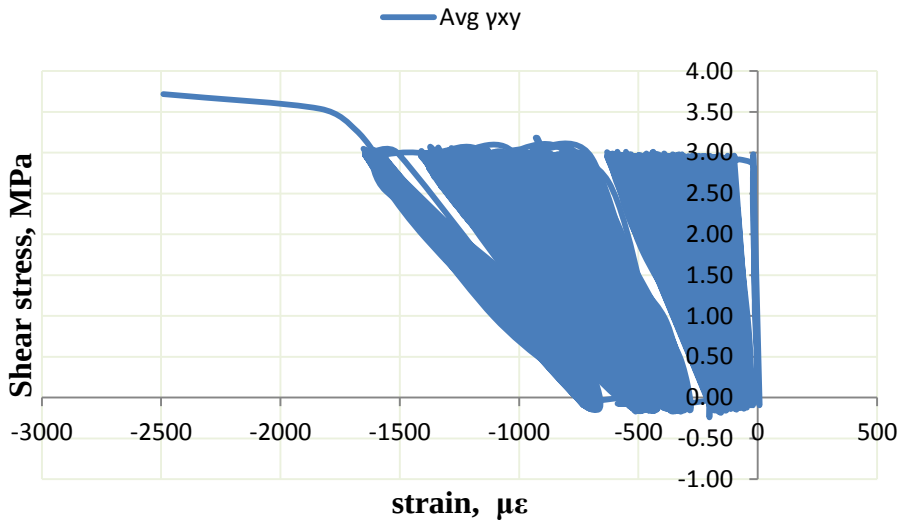



**Figure 4-10: Shear stress – strain curve of specimen DC-70**

### 4.2.4 Comparison amongst the Dry Specimen

Figure 4-11 shows the average strain values of the three species tested under a dry condition with average shear stress at the interface. At lower stress level, the vertical compression strain was dominant and as the stress level was increased, the horizontal tensile strain became dominant for all three specimens. A similar dominant behavior of "crack opening" was observed on a test conducted on a push-off specimen at the University of Porto using transducer measurements (Figuerie, 2015).

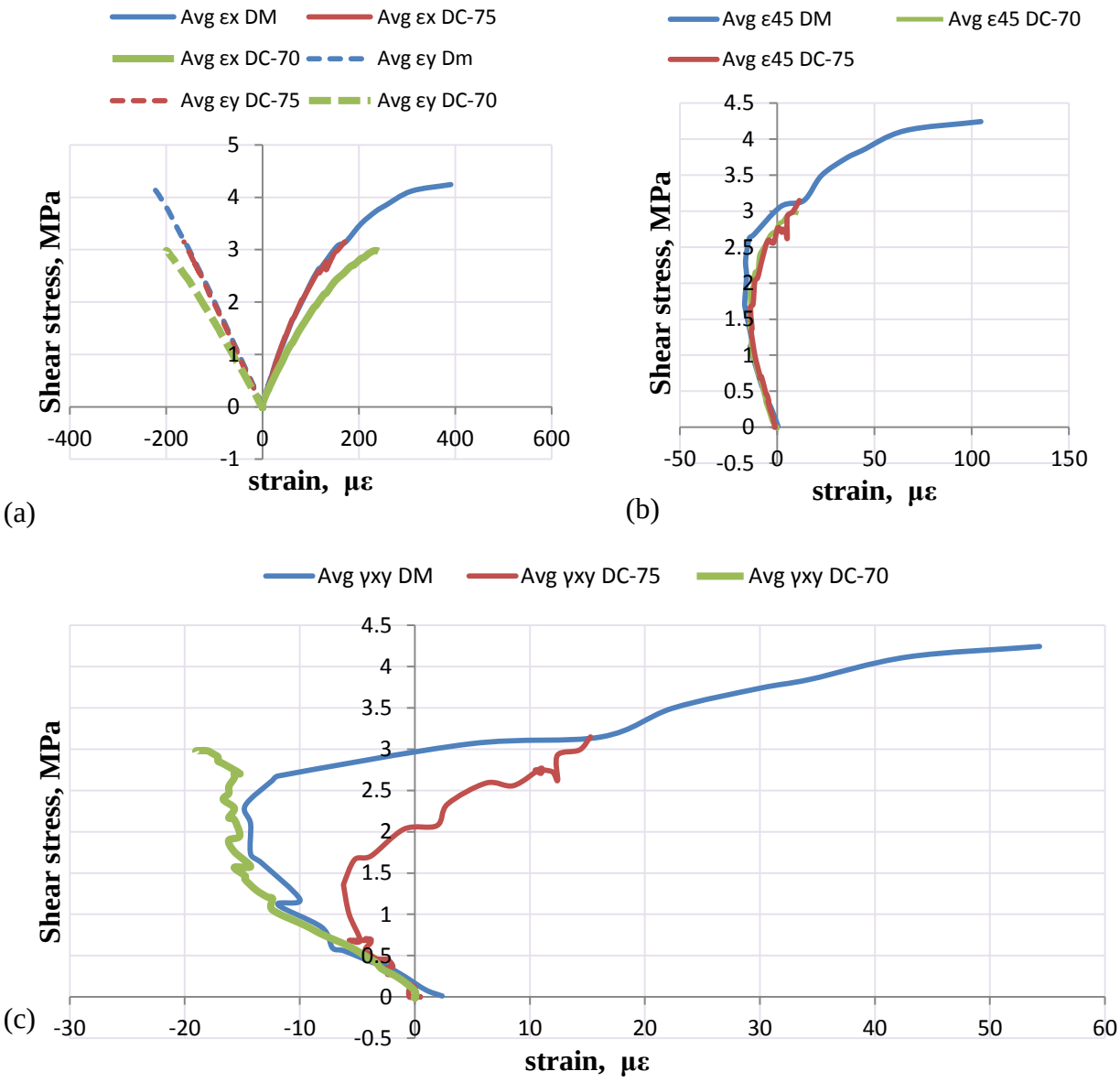



**Figure 4-11: Average shear stress to strain curve of all specimens tested in dry condition. (a) Horizontal and vertical strain; (b) Strain at 45$^{o}$; (c) Shear strain**

It can be seen that for the monotonic tests, the strain right before de-bonding could not be captured. This is because failure was so sudden due to the constantly increasing load. On the other hand, it was possible to observe the failure path of the cyclically loaded specimens. Both cyclic loadings were conducted over a period of four days and loaded not to their ultimate capacity. The vast duration and low amount of load gave the interface a chance to respond to the load. In the loading and unloading process, microcracks propagated through the interface as the number of cycles increased. For instance, the deformation history of specimen DC-75 shows how the horizontal and shear strain had a high rate of increase in peak strain at only one side and how the damage propagated to the other side with a further increase in number of cycles and ultimately reached failure stage (Figure 4-7).

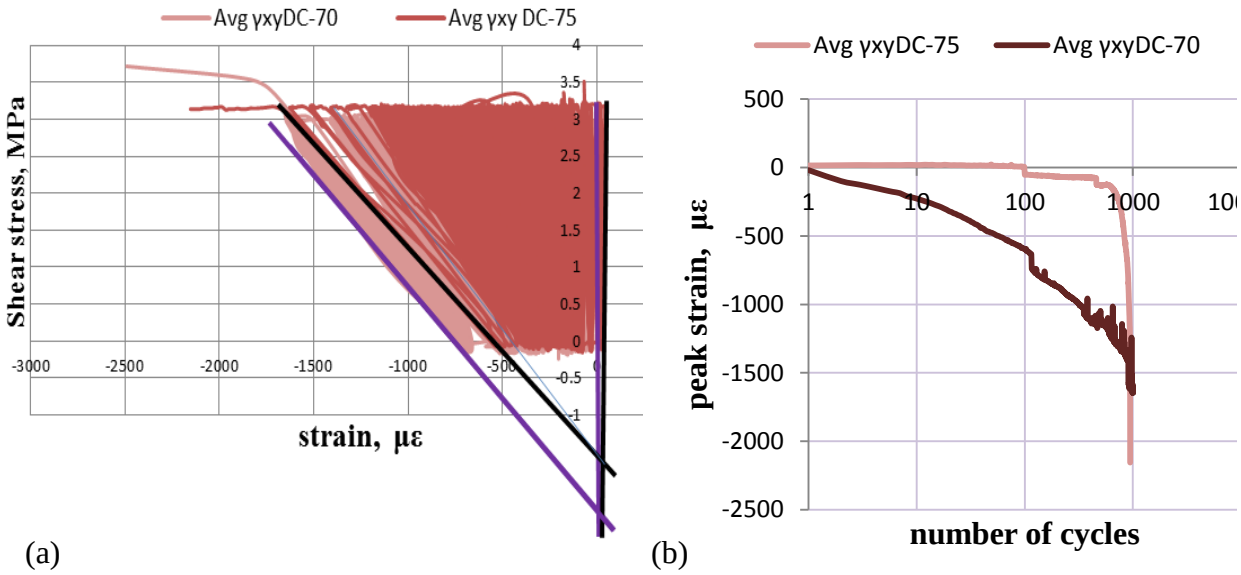


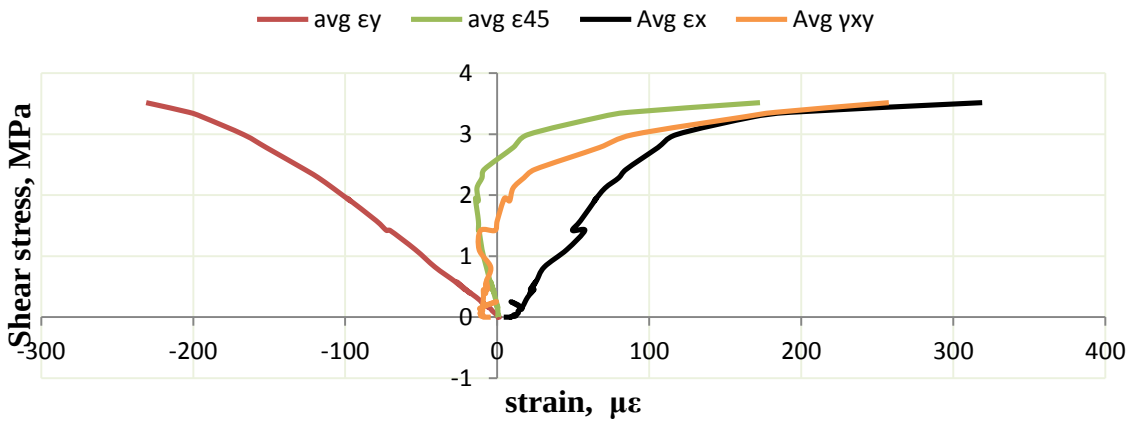

**Figure 4-12: (a) Shear stress – strain curve of all specimens tested in dry condition; (b) Evolution of shear strain with number of cycles of all specimens in dry condition.**

## 4.3 Results of Specimens with the Interface in a Moist Condition

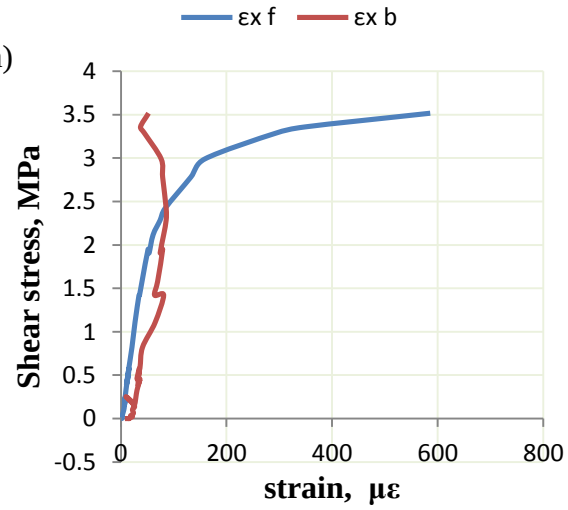
### 4.3.1 Specimen MM

The specimen was tested underwater to investigate if moisture at the interface weakens the interface for a monotonic loading. The specimen showed similar deformation pattern as the specimen tested in dry condition. The specimen failed at 83KN.

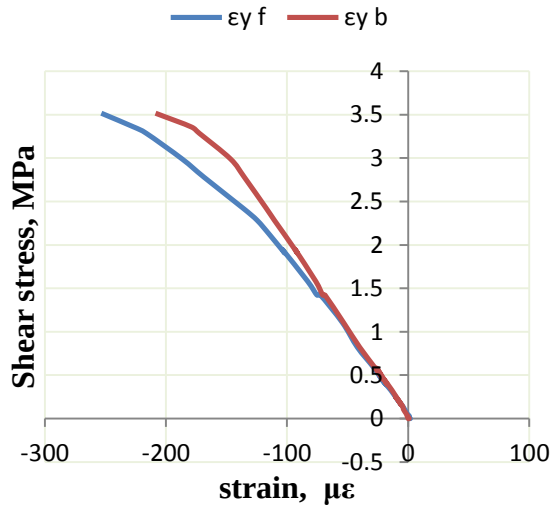
The deformation was localized to the front side of the specimen. The horizontal strain at the back side started decreasing after applying an average shear strain of 2.5MPa at which point the strain at the front side increased with a higher rate as observed in the specimen tested in dry condition (Figure 4-13 (b)). The shear strain value at failure was positive which means the specimen had a deformation as shown in Figure 4-5.



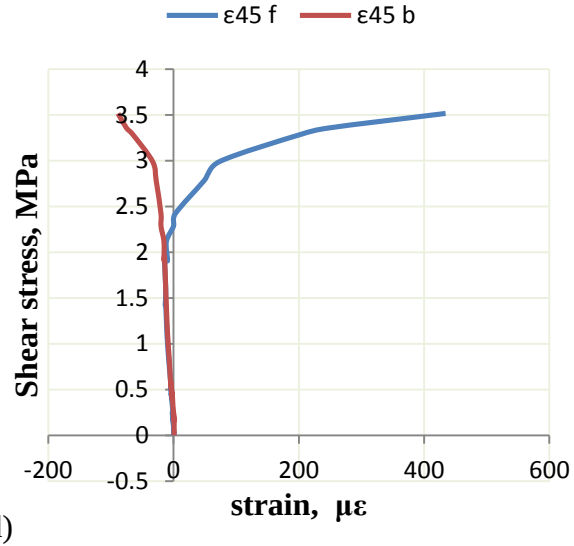

(a)



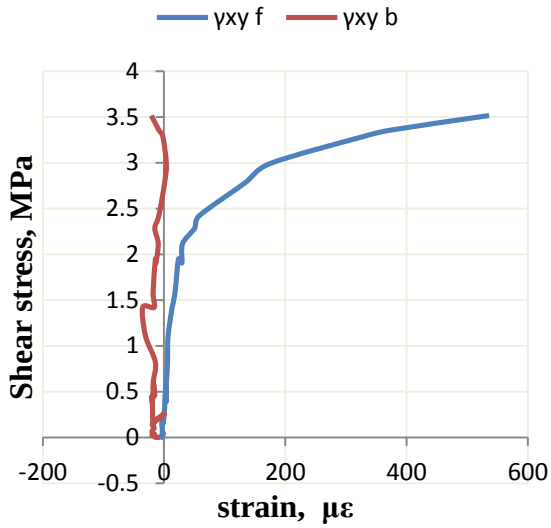

(b)




(c)




(d)




(e)

**Figure 4-13: Average shear stress to strain curve of specimen MM (a) all average strain of the interface; (b) horizontal strain at the front and back side; (c) Vertical strain at the front and back side; (d) strain at an angle of 45$^{o}$ at the front and back side; (e) shear strain at the front and back side**

### 4.3.2 Specimen MC-82

It was planned to load the specimen up to a load corresponding to 85% of the average shear strain of the monotonically loaded specimen since variation in maximum capacity between the specimens cannot be avoided. The specimen was initially loaded to 3Mpa of average shear stress but the strain seemed to be small so the stress was increased to 3.5Mpa after 5 cycles and the cyclic loading was done up to this stress level throughout the test. The shear and the horizontal strain were at 75% and 71% of the monotonically loaded specimen respectively. Here the comparison is made to the dry sample since the deformation pattern of the first cycle of MC-82 specimen was more similar to the dry monotonically loaded specimen. The initial deformation was similar to the other specimens showing the consistency of the sample.

The strain readings showed a typical degradation curve at the beginning of the cycles. A high rate of degradation was observed initially and another increase in rate was observed when the stress was increased to 3.5Mpa. Eventually, the specimen stabilized for all strain readings. Up to the 35$^{th}$ cycle, the shear strain value was positive, indicating a possible eccentric loading. At this point, the horizontal shear strain had reached 0.265‰ which indicates the formation

of microcracks (Figure 4-14 (a)). At the 36th cycle, the specimen formed an unstable crack at the interface and strain readings spiked. The shear strain galloped to the negative value as shown in Figure 4-14 (d). After that, a high rate of degradation with a small increase of number of cycles was observed and the specimen de-bonded at the 44th cycle. The shear strain at failure was 2.5‰.

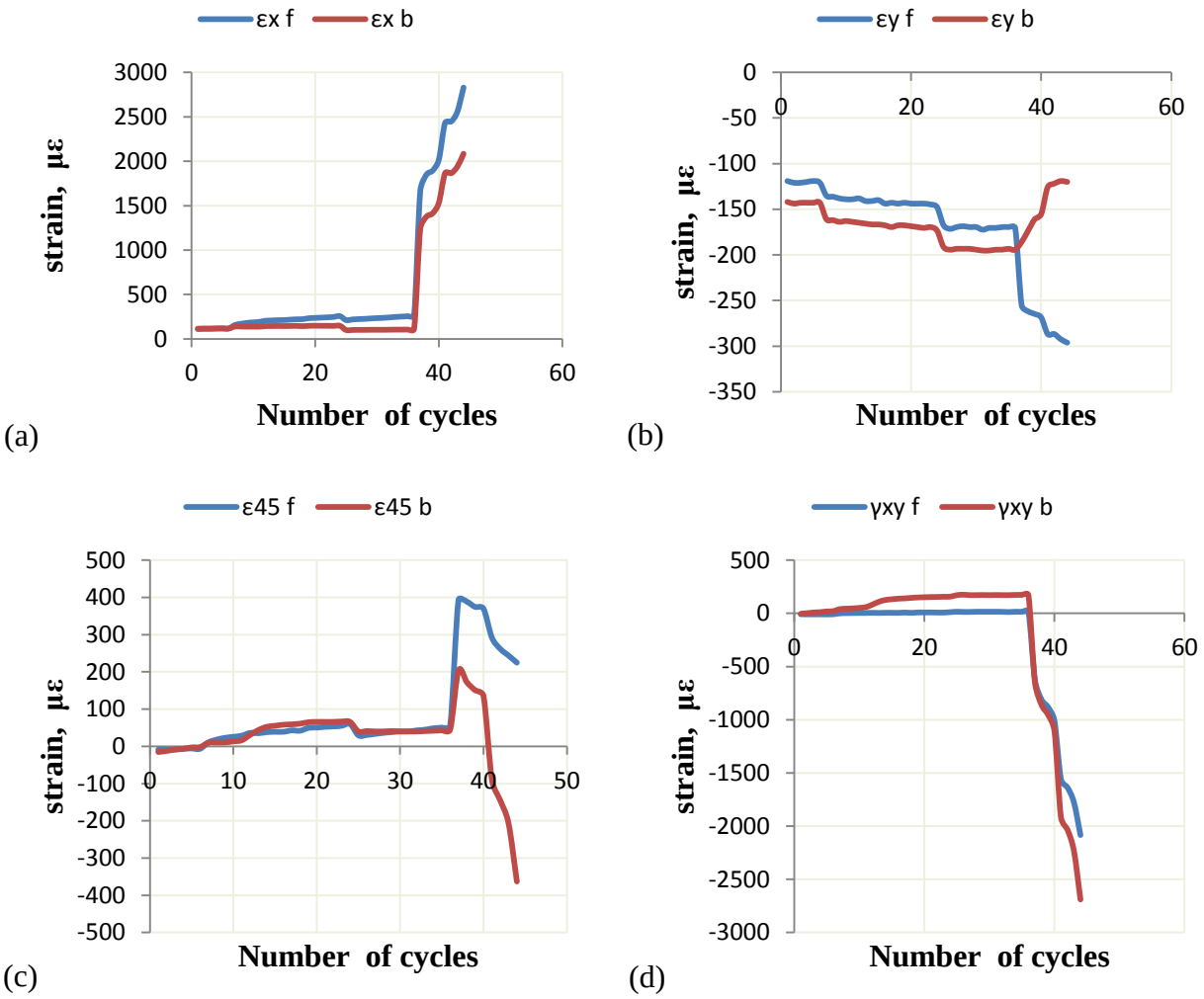



**Figure 4-14: Result of specimen MC-82 (a) Evolution of horizontal strain at the front and back side with number of cycle; (b) Evolution of Vertical strain at the front and back side with number of cycle; (c) Evolution of strain at 45$^{o}$ at the front and back side with number of cycle; (d) Evolution of shear strain at the front and back side with number of cycle**

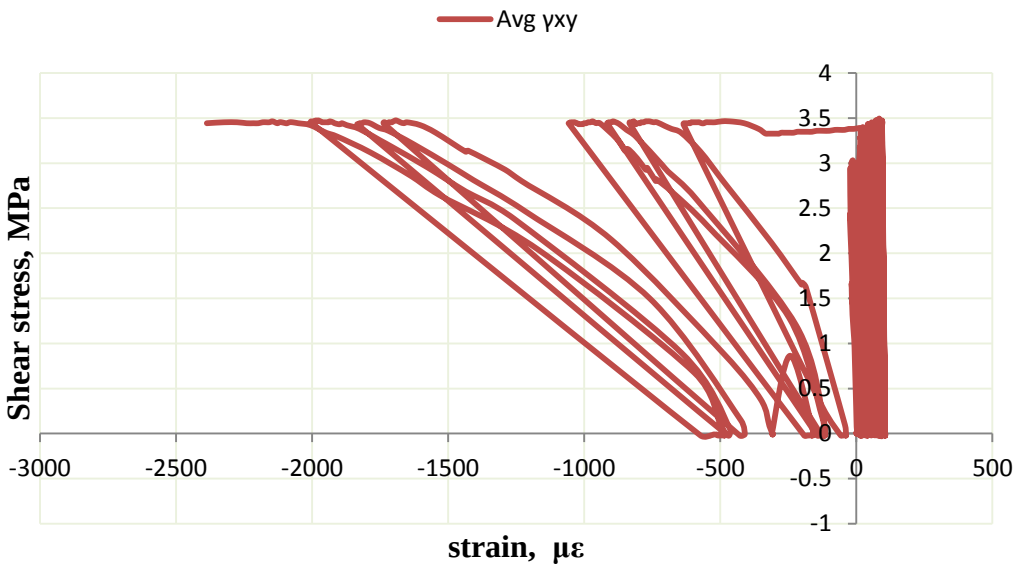



**Figure 4-15: Shear stress – strain curve of specimen MC-82**

### 4.3.3 Specimen MC-60

To study the effect of moisture at a lower load level, the specimen was loaded up to 60KN of load. The deformation pattern was very similar to the other specimens. The shear and the horizontal strain where at 62% and 47.5% of the monotonically loaded dry specimen respectively.

A high initial rate of degradation occurred for the first few cycles and the specimen maintained a reduced level of degradation. At about the 90$^{th}$ cycle unstable cracks formed and the specimen showed a high rate of degradation but rather than progressing to failure, as in the other samples, the specimen stiffened and the rate of degradation reduced again. At about the 290$^{th}$ cycle, unstable cracks formed and the specimen de-bonded at the 301$^{st}$ cycle. At the formation of the first unstable cracks, the horizontal strain had reached 0.53‰.

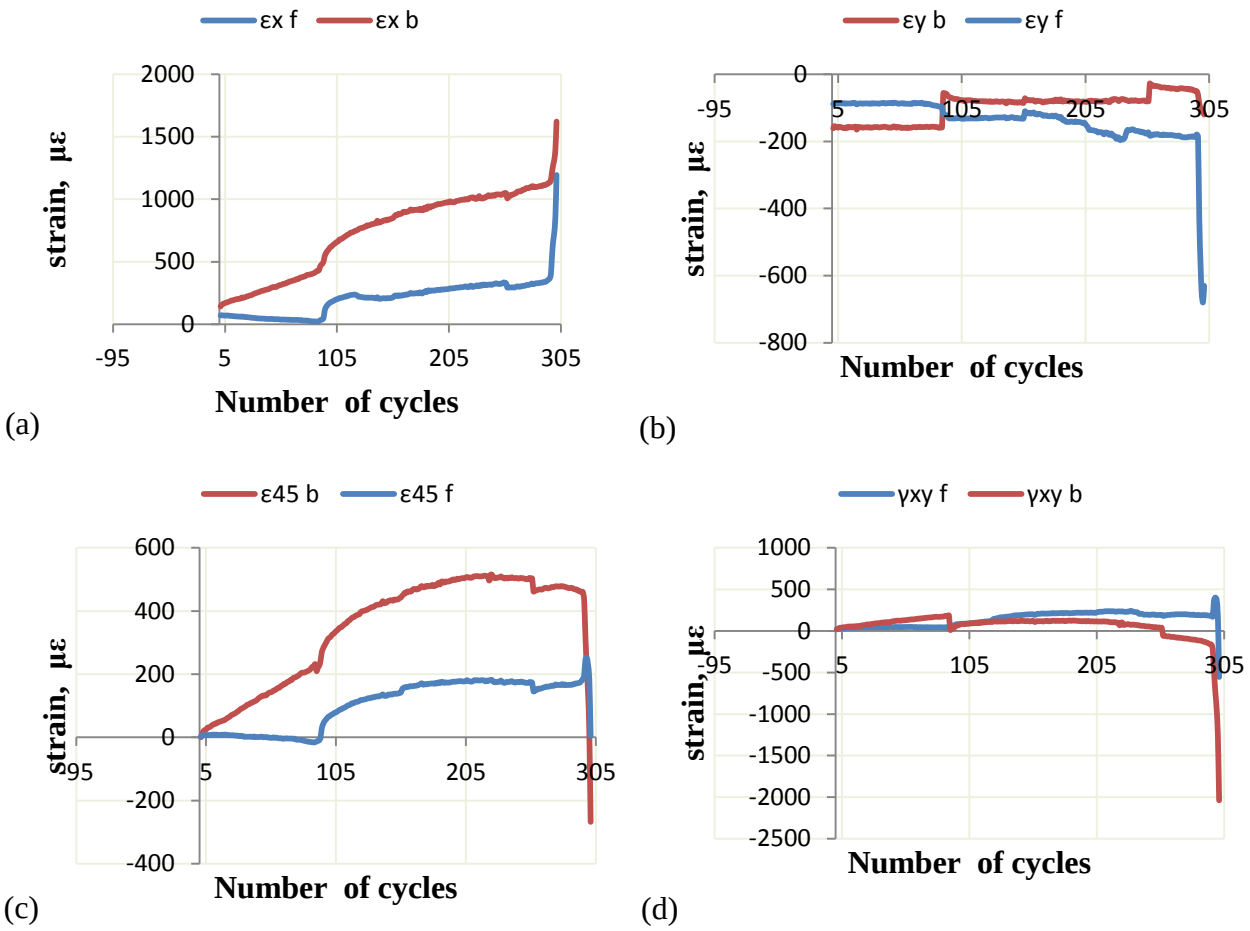



**Figure 4-16: Result of specimen MC-60 (a) Evolution of horizontal strain at the front and back side with number of cycle; (b) Evolution of Vertical strain at the front and back side with number of cycle; (c) Evolution of strain at 45$^{o}$ at the front and back side with number of cycles; (d) Evolution of shear strain at the front and back side with number of cycles**

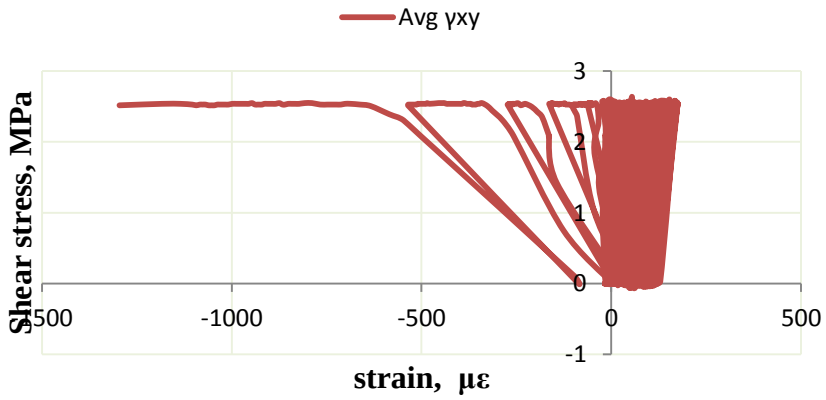



**Figure 4-17: Shear stress – strain curve of specimen MC-60**

### 4.3.4 Comparison amongst the Moist Specimens

The horizontal and vertical strain readings were very similar for all the moist specimens. But the monotonically loaded specimen showed a drastic reduction in stiffness in the horizontal direction and shear deformation (Figure 4-18(c)).

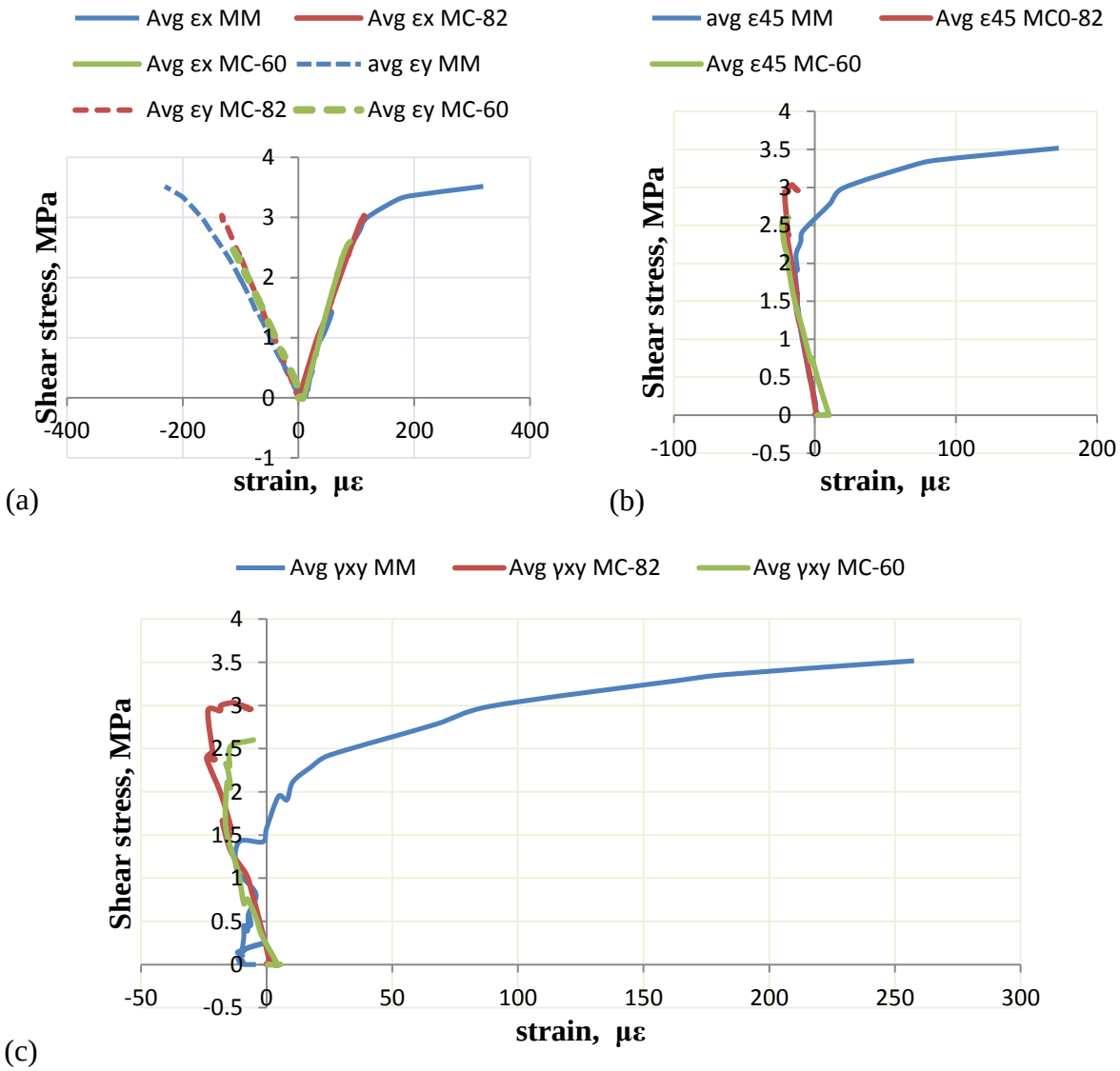
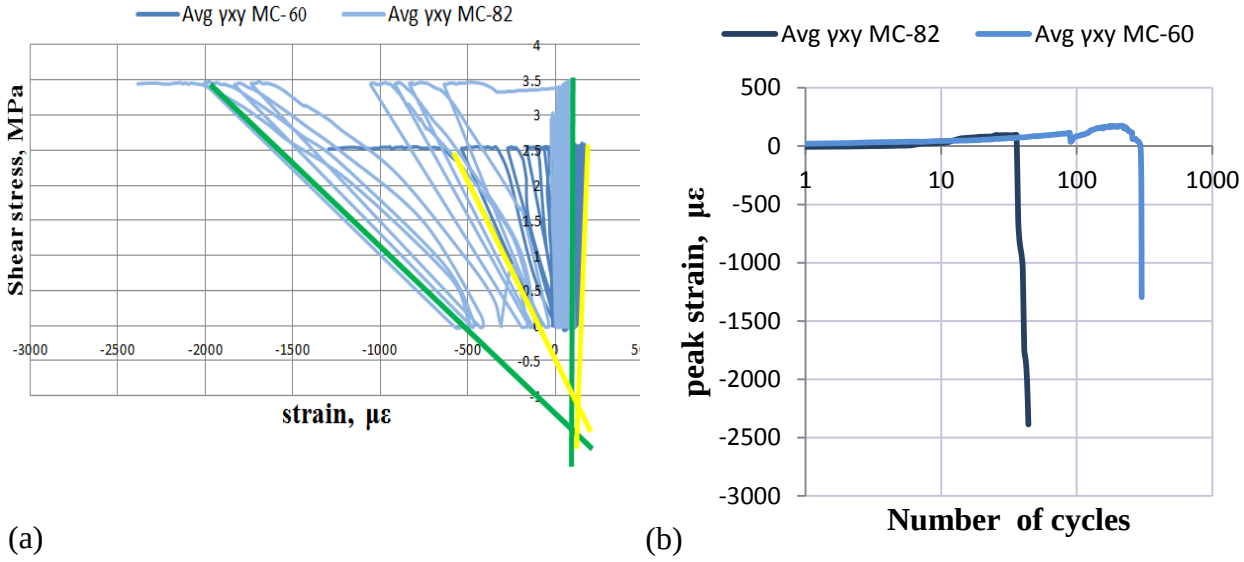



**Figure 4-18: Average shear stress to strain curve of all specimens tested in a moist condition. (a) Horizontal and vertical strain; (b) Strain at 45$^{o}$; (c) Shear strain**

Both the specimens tested for cyclic loading condition showed high stiffness until the formation of microcracks (Figure 4-19). Until this point, the shear strain appeared to be in the positive range far away from the de-bonding strain of the specimen. After the formation of microcracks, the specimens showed a drastic shear deformation increase and the damage

propagation increased from that point on. The damage propagation of the shear strain was very quick for both specimens.




(a) (b)

**Figure 4-19: (a) Shear stress – strain curve of all specimens tested in moist condition; (b) Evolution of shear strain with a number of cycles of all specimens in a moist condition.**

## 4.4 Comparison between the Monolithically Cast Specimens and Specimens with an Interface

The specimens with an interface exhibited reduced shear strength up to 36.6%. Similar behavior has been reported by Zerabruk F. (2015) as well. The shear transfer mechanism in the two cases is different. For an interface with the concrete cast at different times, the adhesive bond between the concretes is significantly reduced. Furthermore, unless the interface is roughened before casting the fresh concrete, the contribution of aggregate interlock is also diminished. The cracked interface of the three sets of samples is presented in Figure 4-20. The surface of the monolithically cast interface is rough with the crack cutting around the aggregates at some points and cutting through it in places where the mortar paste is stronger. The cracked interface of the specimens with an interface is smooth for both dry and moist condition.

Since it was difficult to accurately determine the percentage of loading the cyclic loads were done on, a one to one comparison could not be made between the specimens cast monolithically and the specimens with an interface. A wider experimental program with more number of samples should be conducted to confidently correlate the rate of degradation between the two modes of casting.




**Figure 4-20: (a) Cracked surface of monolithically cast specimens (a) Cracked surface of the specimen with an interface tested in dry condition; (b) Cracked surface of the specimen with an interface tested in moist condition**

## 4.5 Comparison between Moist and Dry Specimens

The specimens loaded in a moist condition showed a higher stiffness or elastic modulus value at lower stress in the horizontal and vertical strain readings (Figure 4-21 (a)). This behavior has been reported in other researches as well (Zheng, D., & Li, X. X., 2011). The stiffening behavior is explained by the pore water pressure developed in the pores of the concrete. At this loading stage, the load is being carried by the concrete and water in the pores of the concrete. Since the specimens were left submerged in water before the test was commenced for about four hours, water is bound to enter some portions of the pores of the concrete. The moisture distribution through the interface was not investigated since it was out of the scope of the research.

At higher stress level in the moist condition, as for the monotonically loaded sample, the stiffness seemed to reduce drastically even below the stiffness of the sample tested in a dry condition (Figure 4-21 (a)). The adverse effect of water on concrete strength has also been reported in different literature (Matsushita, H., & Onoue, K., 2006; T. S. Karanfilov, 1967). With an increase in load, the formation of micro-cracks is inevitable. The adsorbed water in the micro-cracks tends to impose a cleaving action due to the water pressure. This

phenomenon promotes the crack propagation in concrete leading to a reduced stiffness and strength of concrete.

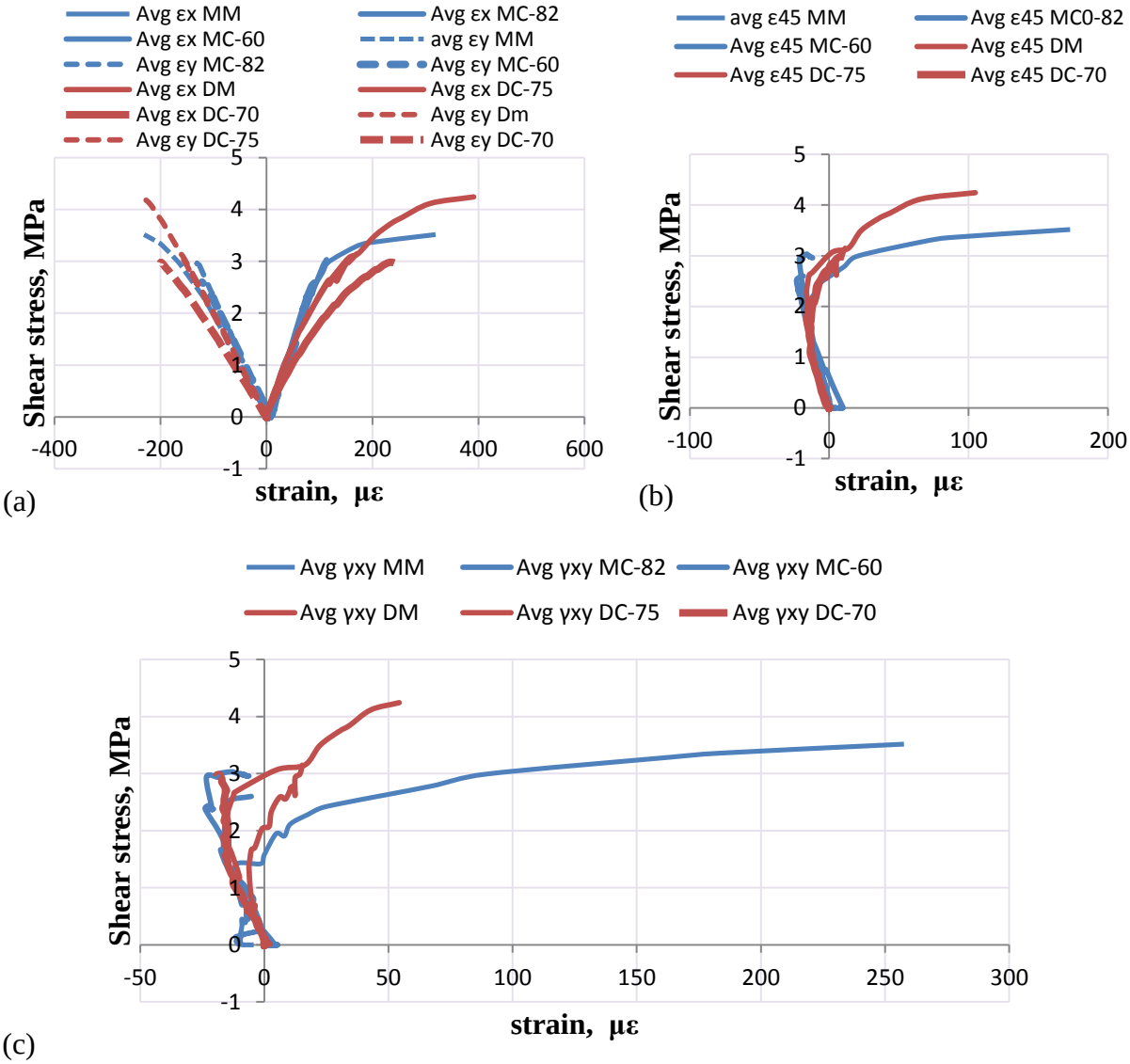
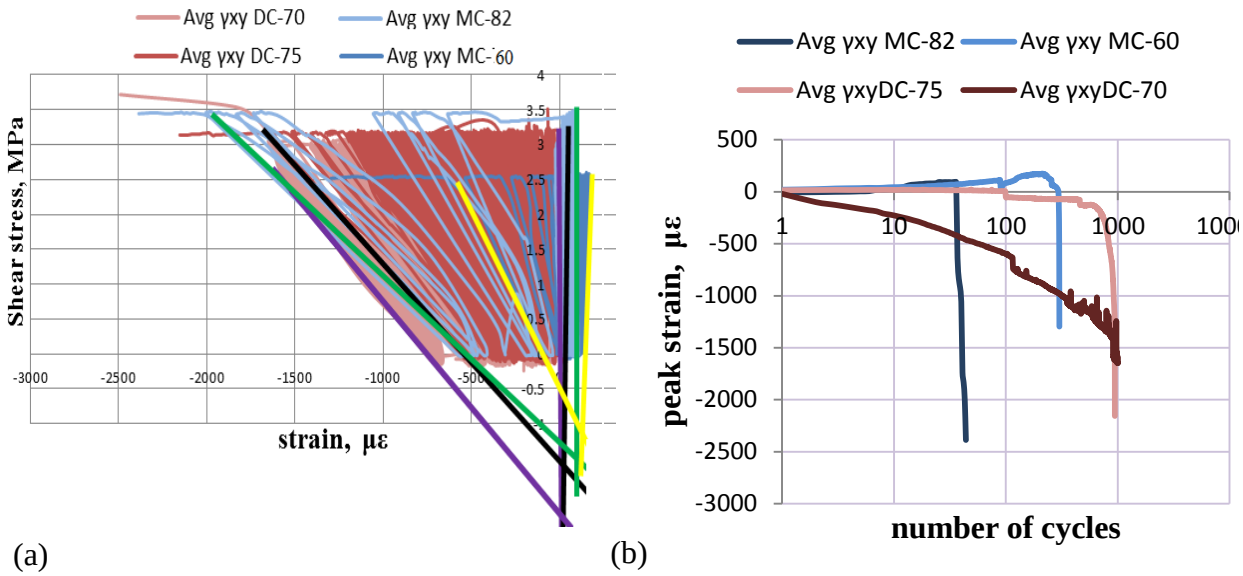



**Figure 4-21: Average shear stress to strain curve of all specimens (a) Horizontal and vertical strain; (b) Strain at 45$^{o}$; (c) Shear strain**

A clear acceleration in degradation of shear strength was observed in the specimens tested in moist condition (Figure 4-22). To preclude any doubt on whether the faster degradation rate was caused by the presence of water, specimen MC- 60 was loaded to a lower stress level than the other specimens. The strain level to which the specimen was loaded is shown in Table 4-2. Even at this load level, the specimen could only sustain 300 cycles of load.

At the initial cycles of loading, a stiffer shear resistance is observed due to the contribution of pore water pressure in the load transfer process (Figure 4-22 (b)). With increasing number of cycles and formation of micro-cracks, the pore water pressure promotes the propagation of the micro-cracks.

In addition to promoting the propagation of micro-cracks, water also has a lubricating effect on the surface of the microcracks. The internal friction that is developed between the surfaces of the micro-cracks is compromised due to the presence of water further contributing to the acceleration of degradation of the interface (T. S. Karanfilov, 1967).




(a) (b)

**Figure 4-22: (a) Shear stress – strain curve of all specimens; (b) Evolution of shear strain with number of cycles of all specimens.**

## 4.6 Summary of the Experimental Result

The results of the experiment are summarized in Table 4-1and Table 4-2. For the cyclic tests, the specimens were fully unloaded. It was not possible to retain a minimum load since the load was applied manually with a hydraulic jack. For this reason, only the peak load of the cyclically loaded specimens is presented in the summary.

**Table 4-1: Results of monolithically cast specimens**

| Casting condition | Specimen designation | Loading condition | Load | # of cycles to failure |
|---|---|---|---|---|
| monolithic | MD-M | monotonic | 131KN | - |
| | MDC-110 | cyclic | 110KN | 4 |
| | MDC-92 | cyclic | 92KN | 1000+ |

**Table 4-2: Results of specimens with an interface**

| condition | specimen designation | loading condition | Load (KN) | %age from average $\varepsilon_y$ [1] of the dry monotonic specimen | %age from average shear of the dry monotonic specimen | %age from average $\varepsilon_x$ [2] of the dry monotonic specimen | %age with ultimate dry load | # of cycles to failure |
|---|---|---|---|---|---|---|---|---|
| dry | DM | monotonic | 100 | | - | - | | - |
| | DC-75 | cyclic | 75 | 75% | 75% | 75% | 75% | **994** |
| | DC-70 | cyclic | 70 | 70% | - | 85.50% | 70% | **1000 +** |
| wet | MM | monotonic | 83 | | - | - | | - |
| | MC-82 | cyclic | 82 | 68.40% | 75% | 71% | 82% | **44** |
| | MC-60 | cyclic | 60 | 56.60% | 62% | 47.50% | 60% | **301** |

[1] *strain in the vertical direction* [2] *strain in the horizontal direction*

# 5 FINITE ELEMENT MODELING

## 5.1 About the Software

The analytical simulation of the push-off specimen was done on non-linear finite element software called DuCOM-COM3. This program was developed at the University of Tokyo. The program is an integral of the two simulation tools, DuCOM and COM3. DuCOM for stands for Durability Models of Concrete and traces the development of concrete hardening (hydration), structure formation and several associated phenomena, from casting of concrete to a period of several months or even years while COM3 is a three-dimensional finite element simulating tool.

The program is capable of capturing the behavior of structures incorporating the effect of ingredient materials and environmental condition. The platform has been proven to give results that fairly agree with experimental outputs in numerous research.

## 5.2 Specimens Modeled

A push-off specimen with and without an interface was modeled along with the confining bars. At this stage, monotonic loading condition and dry environmental condition is considered because strong model to capture the behavior of construction joints and water in concrete is still rudimentary.

## 5.3 Modeling the Specimens

### 5.3.1 Concrete:

A mean value of compressive strength was taken from the cube tests conducted. The modulus of elasticity and tensile strength were obtained from Eurocode 2 corresponding to the obtained compressive strength.

**Table 5-1: Properties of concrete used in the model**

| | |
|---|---|
| **Initial stiffness** | 33.5Gpa |
| **cylindrical compressive strength** | 40MPa |
| **Tensile strength** | 3.5Mpa |
| **Poisson's ratio** | 0.2 |

### 5.3.2 Reinforcement:

The reinforcement layout for the internal bars is shown in Figure 5-1. It is simulated as smeared reinforcement by providing the reinforcement ratio in the concrete element. The reinforcement does not have any effect on the behavior of the interface aside from preventing failure at the top and sides of the concrete parts.

**Table 5-2: Reinforcement property used in the model**

| | Internal bar | External bars |
|---|---|---|
| **Initial stiffness** | 210GPa | 210Gpa |
| **Yield strength** | 520Mpa | 350MPa |
| **Ultimate strength** | 600Mpa | 350MPa |

### 5.3.3 Bond Element

For the specimens with a construction joint, a bond element was modeled as shown in Figure 5-1. A plastic softening model is used to model the bond element. The model has been used to represent the behavior of steel-concrete interface. From comparisons of the model with other experimental programs, the model captures peak load and deformation adequately (Maekawa, K., Okamura, H., & Pimanmas, A., 2003).

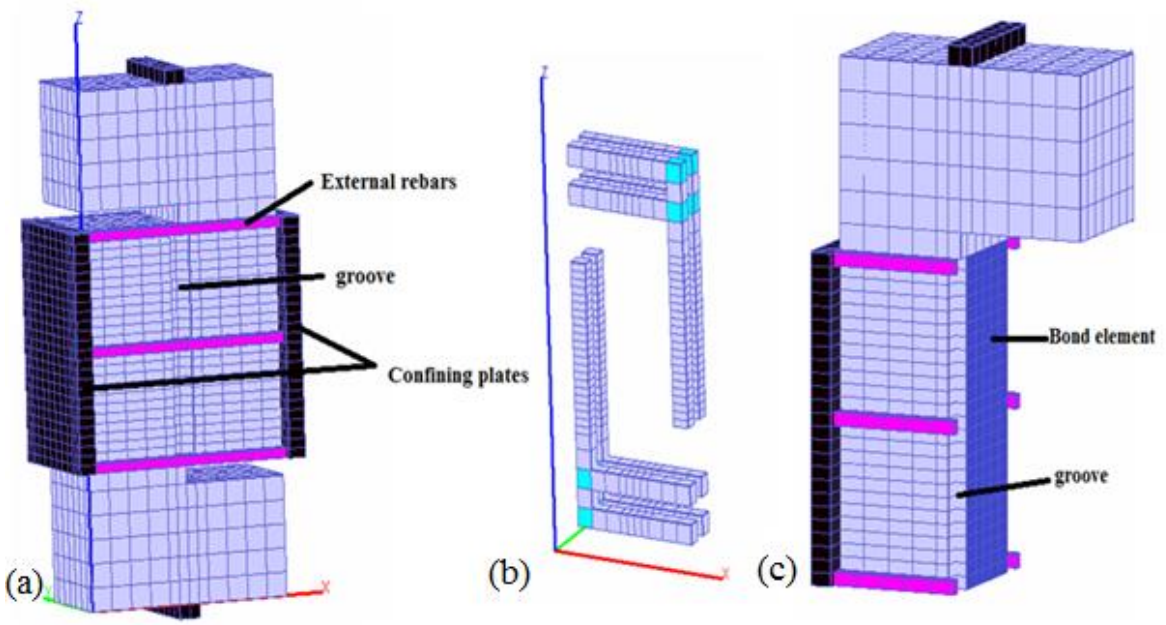



**Figure 5-1: (a) Model of the entire specimen; (b) Internal reinforcement layout; (c) Bond element for specimens with an interface.**

The input parameters for the model are shear fracture energy, open fracture energy, initial cohesive shear strength, initial tensile strength in open mode, confining stress from which dilatancy is 0 and tangent of frictional angle. The parameters used are stated in .

**Table 5-3: Bond element parameters**

| | |
|---|---|
| **Shear Fracture Energy, N/mm** | 0.002 |
| **Open Fracture Energy, N/mm** | 0.01 |
| **Initial Cohesive Shear Strength, MPa** | 2 |
| **Initial Tensile Strength in Open Mode, MPa** | 1.75 |
| **Confining Stress from Which Dilatancy is 0, MPa** | 0 |
| **Tangent of Frictional Angle** | 0.9 |

It is important to point out that sufficient data is not present to model construction joints. While some parameters were inferred from literature, some parameters were iterated depending on the current experimental program. The fracture energy parameters majorly affect the post-peak behavior since the parameters represent the amount of energy needed for crack propagation. Fracture energy for tension was taken as 0.01 considering the brittle nature of concrete under tension (Maekawa, K., Okamura, H., & Pimanmas, A., 2003). The initial cohesive shear strength of the interface is the shear strength of the interface without the effect of confinement. A value less than the one obtained from the experiment was used. A significant reduction in tensile strength was obtained for concrete with an interface in literature (Julio, E. N. B. S., 2004).For the initial tensile strength, a value half the tensile strength of concrete was used for the interface. The confining stress for which dilatancy is zero was taken as zero, in other words, dilatancy was not considered. This was done with the reasoning that the surface was left as cast after vibration, which left the surface to be fairly smooth. The tangent of frictional angle was taken as 0.9 from literature (M.E Mohamad, 2014; Devia, A. K., 2015).

### 5.3.4 Support Condition

The nodes at the bottom of the push –off specimen were pinned allowing rotation about the support. The nodes at the top were also pinned and a downward vertical displacement was applied.

## 5.4 Results of the Monotonically Loaded Specimen

As shown in Figure 5-2 the local ultimate load of the specimen before and after de-bonding was captured by the model with sufficient accuracy.

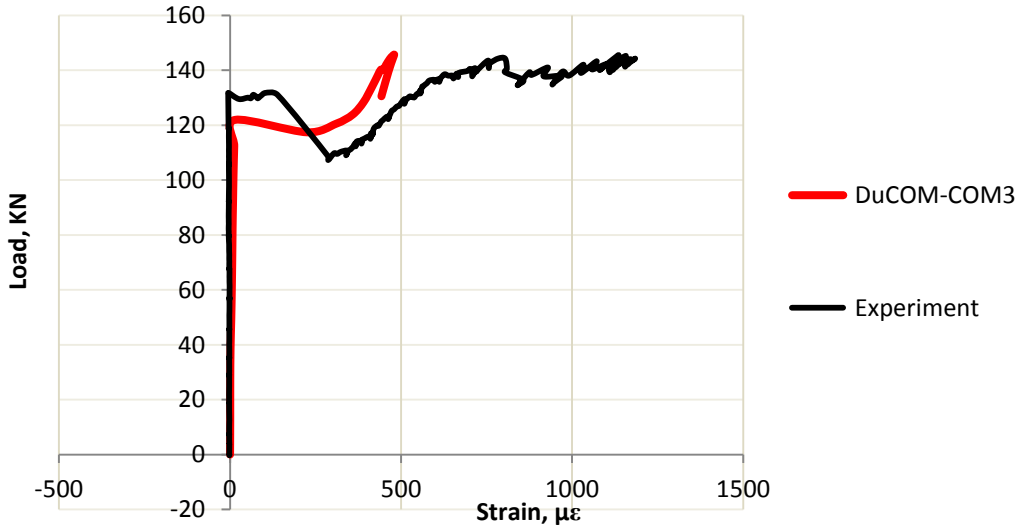



**Figure 5-2: Average tensile strain of confining bars (experimental Vs DuCOM-COM3)**

## 5.5 Results of the Specimen with an Interface

Even though there is limited data available, a rough envelope from the results of the specimen is prepared in Figure 5-3. The failure strain of the monotonically loaded specimen was not captured due to the sudden failure of the specimens. The failure shear strain of the cyclically loaded specimen is utilized to prepare the envelope. The peak stress of the envelope is taken from the specimen tested in dry condition for monotonic loading.

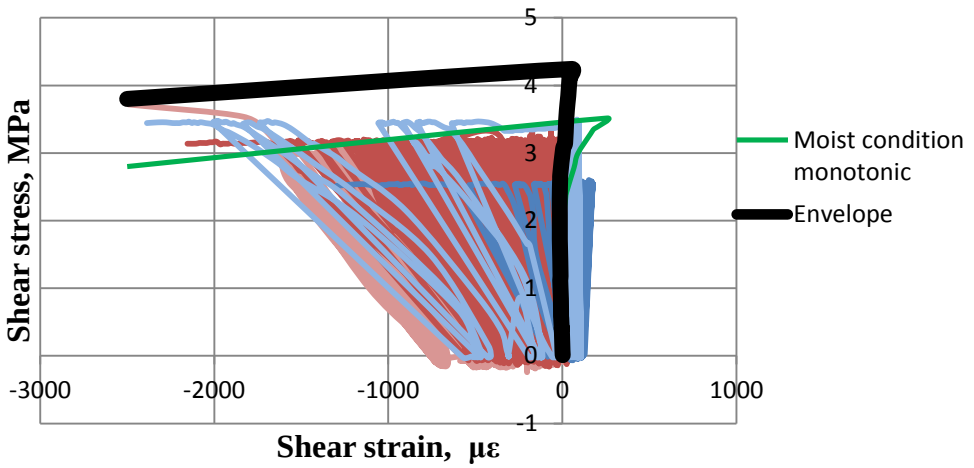



**Figure 5-3: Failure envelope**

With the interface parameters used, the model captured the de-bonding strength with adequate accuracy.

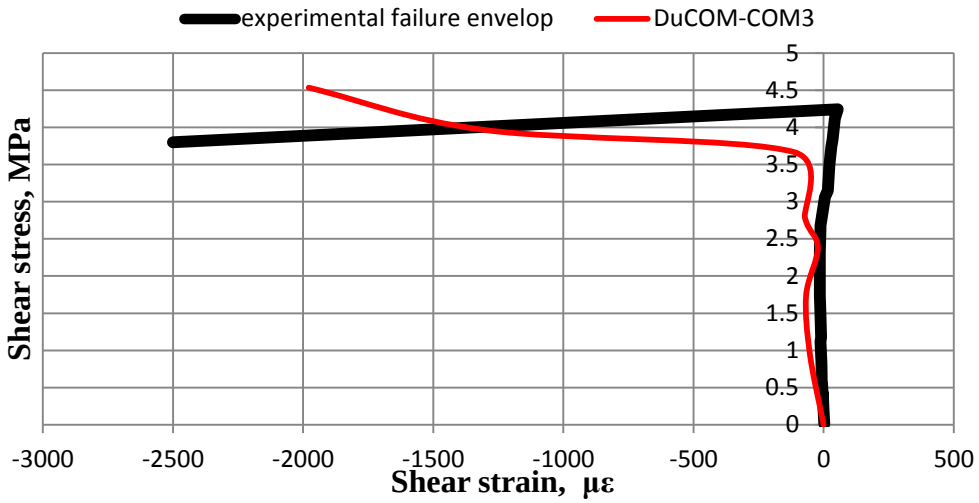



**Figure 5-4: Comparison of experimental and model results of the monotonically loaded specimen**

# 6 CONCLUSION AND RECOMMENDATION

## 6.1 Conclusions

In this paper, a modified instrumentation scheme was used on a push-off specimen in an experimental program to investigate the degradation nature of an interface created when concrete is cast at different times for cyclic shear loading under dry and moist condition. Three strain gauges were placed on each side of the interface in three different directions from which shear strain was calculated.

The following conclusions are made from the experimental and analytical observation in the research.

- It was possible to capture the deformation at the interface before de-bonding using strain gauges. The dominant continuum behavior of the interface could not be represented well with the use of LVDT measurements
- The experimental program indicated that the presence of water pronouncedly accelerated the degradation of the interface for cyclic loading. Even with cyclic loading at a lower amplitude of loading than the specimens tested in a dry condition, de-bonding of the interface occurred in fewer cycles. This adverse effect of water was not apparent both at initial number of cycles and lower load levels, rather a stiffening effect was observed possibly due to the development of pore water pressure.
- The existence of a joint at the interface seemed to drastically reduce the shear transfer capacity. A reduction of capacity up to 36.6% was observed. A solid conclusion could not be made on the difference of degradation nature of concrete with and without an interface with the limited number of specimens tested.
- Possible parameters to model construction joints are suggested using DuCOM-COM3 based on the experimental program conducted. The model fairly predicted the peak load.

## 6.2 Recommendation

- Due to the shear strength weakening nature of construction joints on a structure and given their inevitability, a strive should be made to understand the nature of these joints with sufficient accuracy. Aside from the behavior of these interfaces in shear, their property in tension and compression should be a subject of study as well, to come up with a model to represent their behavior.
- The environmental condition should not be abandoned as the exposure to water greatly accelerated the degradation process of the interface. Considering structures like bridge piers submerged in water, bridge decks exposed to heavy flood and water retaining structures, the effect of presence of water should not be overlooked and further works should be done to come up with an appropriate model to adequately capture the behaviour and put out a safe design of members with an interface exposed to prolonged moisture condition.
- For future research, the damage per cycle should be quantified in dry and moist condition of the interfaces in a larger scale program. Contribution should be made towards creating design friendly methods for the construction industry considering the effect of the environmental conditions.
- Even though a reasonable simulation was made with the finite element model for the specimen under consideration, the model should be investigated for joints at member and structure level. Further works are commencing regarding this area.

# REFERENCE

Bass, R. A., Carrasquillo, R. L., & Jirsa, J. O. (1989). Shear transfer across new and existing concrete interfaces. *Structural Journal*, *86*(4), 383-393.

Birkeland, P. W., & Birkeland, H. W. (1966, March). Connections in precast concrete construction. In *Journal Proceedings* (Vol. 63, No. 3, pp. 345-368).

Casal, B. B. (2011). Connections between Concrete Layers with Different Ages. *Universidade Tecnica de Lisboa: Lisboa, Portugal*, 1-10.

Constantinescu, H., & Magureanu, C. (2011). Study of shear behaviour of high Performance concrete using push-off tests. *Civil Engineering and Installations*.

Devia, A. K., srinivas, V., & Ramanjaneyuluua, K. (2015, March). Evaluation of Interfacial Shear Strength in Concrete Composite Construction using Nonlinear Finite Element Analysis. *In National Conference on technological Innovations for Sustainable Infrastructure* (Vol. 13, p.14).

Figueira, D., Sousa, C., Calçada, R., & Neves, A. S. (2015). Push-Off Tests in the Study of Cyclic Behavior of Interfaces between Concretes Cast at Different Times. *Journal of Structural Engineering*, *142*(1), 04015101.

Gebreyouhannes, E., Kishi, T., & Maekawa, K. (2008). Shear fatigue response of cracked concrete interface. *Journal of Advanced Concrete Technology*, *6*(2), 365-376.

Hofbeck, J. A., Ibrahim, I. O., & Mattock, A. H. (1969, February). Shear transfer in reinforced concrete. In *Journal Proceedings* (Vol. 66, No. 2, pp. 119-128).

Hsu, T. T., Mau, S. T., & Chen, B. (1987). Theory on shear transfer strength of reinforced concrete. *Structural Journal*, *84*(2), 149-160.

Isojeh, B., El-Zeghayar, M., & Vecchio, F. J. (2017). Concrete damage under fatigue loading in uniaxial compression. *ACI Mater. J*, *114*(2), 225-235.

Julio, E. N. B. S., Branco, F. A., & Silva, V. D. (2004). Concrete-to-concrete bond strength. Influence of the roughness of the substrate surface. *Construction and Building materials*, *18*(9), 675-681.

Júlio, E. N. B. S., Dias-da-Costa, D., Branco, F. A. B., & Alfaiate, J. M. V. (2010). Accuracy of design code expressions for estimating longitudinal shear strength of strengthening concrete overlays. *Engineering Structures*, *32*(8), 2387-2393.

Kaji, T., & Fujiyama, C. (2014). Mechanical properties of saturated concrete depending on the strain rate. *Procedia Engineering*, *95*, 442-453.

Karanfilov, T. S. (1967). Fatigue of water-saturated concrete. *Hydrotechnical Construction*, *1*(9), 798-800.

Maekawa, K., Okamura, H., & Pimanmas, A. (2003). *Non-linear mechanics of reinforced concrete*. CRC Press.

Mattock, A. H. (1960). *Shear transfer under monotonic loading across an interface between concretes cast at different times*. Department of Civil Engineering, University of Washington.

Mattock, A. H. (1977). *Shear Transfer Under Cyclically Reversing Loading Across an Interface Between Concretes Cast at Different Times*. Department of Civil Engineering, University of Washington.

Matsushita, H., & Onoue, K. (2006). Influence of surface energy on compressive strength of concrete under static and dynamic loading. *Journal of Advanced Concrete Technology*, *4*(3), 409-421.

Mohamad, M. E., Ibrahim, I. S., Abdullah, R., Rahman, A. A., Kueh, A. B. H., & Usman, J. (2015). Friction and cohesion coefficients of composite concrete-to-concrete bond. *Cement and Concrete Composites*, *56*, 1-14.

Pimanmas, A., & Maekawa, K. (2001). Influence of pre-crack on RC behavior in shear. *Doboku Gakkai Ronbunshu*, *2001*(669), 277-291.

Rahal, K. N., & Al-Khaleefi, A. L. (2015). Shear-Friction Behavior of Recycled and Natural Aggregate Concrete-An Experimental Investigation. *ACI Structural Journal*, *112*(6), 725.

Rahal, K. N., Khaleefi, A. L., & Al-Sanee, A. (2016). An experimental investigation of shear-transfer strength of normal and high strength self-compacting concrete. *Engineering Structures*, *109*, 16-25.

Ross, C. A., Jerome, D. M., Tedesco, J. W., & Hughes, M. L. (1996). Moisture and strain rate effects on concrete strength. *Materials Journal*, *93*(3), 293-300.

Santos, P. M., & Julio, E. N. (2007). Correlation between concrete-to-concrete bond strength and the roughness of the substrate surface. *Construction and Building Materials*, *21*(8), 1688-1695.

Santos, P. M. D., & Júlio, E. N. B. S. (2011). Factors affecting bond between new and old concrete. *Materials Journal*, *108*(4), 449-456.

Santos, P. M., & Júlio, E. N. (2014). Interface shear transfer on composite concrete members. *ACI Structural Journal*, *111*(1), 113.

Van Mier, J. G. M., Ruiz, G., Andrade, C., & Yu, R. C. UPGRADING THE PUSH-OFF TEST TO STUDY THE MECHANISMS OF SHEAR TRANSFER IN FRC ELEMENTS.

Vintzeleou, E. N., & Tassios, T. P. (1987). Behavior of dowels under cyclic deformations. *Structural Journal*, *84*(1), 18-30.

Walraven, J. C. (1980). "Aggregate interlock: A theoretical and experimental analysis," *thesis presented to Delft University of Technology, at Delft, Netherlands, in partial fulfillment of the requirements for the Degree of Doctor of Philosophy.*

Walraven, J. C., Vos, E., and Reinhardt, H. W . (1979). Experiments on shear transfer in cracks in concrete. Part I: Descriptions of results. *Stevin Report 5-79-3, Delft University of Technology*., Delft, Netherlands.

Zerabruk F. (2015). Experimental investigation of construction joints in RC beams. *Thesis presented to Addis Ababa University Institute of technology, at Addis Ababa, Ethiopia*, in Partial Fulfilment of the Requirements for the Degree of Master of Science.

Zheng, D., & Li, X. X. (2011). Microcrack evolution and stress-strain relationship of saturated concrete. In *Advanced Materials Research* (Vol. 243, pp. 4462-4465). Trans Tech Publications.